Product: ZVK

Measurement Accuracy of the
ZVK
Vector Network Analyzer

Application Note

Measurement deviations due to systematic errors of a network analysis system can be drastically reduced by an appropriate system error calibration. After system error correction, the residual measurement uncertainties are - besides the stability, linearity, and dynamic range of the network analyzer system - mainly affected by the quality of the calibration standards and the repeatability of the connections. The effective measurement accuracy of the network analysis system can be determined using the results of successive verification measurements utilizing highly precise verification standards.

ROHDE & SCHWARZ

Contents

1   Abstract

Measurement deviations due to systematic errors of a network analysis system can be drastically reduced by an appropriate system error calibration. After system error correction, the residual measurement uncertainties are - besides the stability, linearity, and dynamic range of the network analyzer system - mainly affected by the quality of the calibration standards and the repeatability of the connections. The effective measurement accuracy of the network analysis system can be determined using the results of successive verification measurements utilizing highly precise verification standards.

2   Calibration

For the calibration of the network analyzer for the whole frequency range up to 40 GHz, a coaxial calibration kit model 8770N03 (made by Maury Microwave corporation, USA) with 2.92 mm connectors was used. This type of calibration kit is also directly available from Rohde & Schwarz (Calibration Kit ZV-Z35, R&S order no. 1128.3547.02). It contains several calibration standards;

- **O**PEN circuits

- **S**HORT circuits

- **M**ATCH standards.

The characteristic data of the standards (electrical lengths and coefficients for the fringing capacitance of the OPENS) are stored on a floppy disk which is part of the calibration kit. For achieving a high effective directivity for frequencies greater than 4 GHz, two sliding MATCHES (also called sliding terminations or sliding loads) are included.

In addition, the ZVK was calibrated by means of a 3.5 mm calibration kit 85052B (made by Agilent Technologies, USA). The greater diameter of the outer conductor (3.5 mm compared to 2.92 mm) facilitates an even higher precision of the standards, resulting in a further improved accuracy. Unfortunately, 3.5 mm standards are limited to an upper frequency of 26.5 GHz.

Two test cables of type FD0BS0HR025.0 (made by W. L. Gore & Associates, USA) were connected to the test ports of the analyzer. The cables comprise special rugged connectors - resulting in a mechanically very stable connection to the network analyzer - and precise 2.92 mm male connectors to connect to the devices under test (DUT). For the 3.5 mm measurements, adapters from the 85052B calibration kit were directly connected to the cables, to form the new 3.5 mm reference planes. All measurements were performed in a laboratory without an air-conditioning system.

Out of the great variety of calibration techniques the ZVK offers, the TOM method (R&S patent) was chosen. It is simple to carry out, precise, and moreover, it allows the simultaneous operation of one male and one female test port. This is advantageous for successive verification procedures as all the verification standards show one male and one female connector.

3   Verification

To verify the residual measurement uncertainties of the network analyzer after system error correction with 2.92 mm connectors, the Anritsu K verification kit model 3668 was applied. It contains four verification standards;

- a matched homogeneous 50 Ω airline

- a matched attenuator with 20 dB attenuation

- a matched attenuator with 50 dB attenuation

- a mismatched stepped 50 Ω airline containing a 25 Ω section (Beatty standard).

For all four verification standards, the diameter of the outer conductor is 2.92 mm. Their S-parameters were measured by the manufacturer as precisely as possible. As stated by the manufacturer: *"The components in the kits are of the highest quality and accuracy. All components are NIST (National Institute of Standards and Technology of the USA) traceable, which means that the components are very accurate and repeatable."*

The measurement data together with the corresponding uncertainties are delivered by the manufacturer as a verification report on a floppy disk. As an example, the data of the standards for the highest frequency (40 GHz) is shown in the following tables (Table 3-1: magnitude data; Table 3-2: phase data).

Table 3-1   Reported **magnitude** data and magnitude uncertainties of the **2.92 mm** verification standards at 40 GHz

Verification	S11		S21		S12		S22	
Standard	MAG lin	UNC +/-	MAG /dB	UNC +/-	MAG /dB	UNC +/-	MAG lin	UNC +/-
50 Ω	.006	.010	-0.204	.154	-0.200	.154	.008	.010
20 dB	.078	.010	-19.989	.154	-19.982	.154	.085	.010
50 dB	.037	.010	-49.593	.424	-49.602	.424	.128	.010
25 Ω	.585	.054	-2.137	.154	-2.140	.154	.584	.054

Table 3-2   Reported **phase** data and phase uncertainties of the **2.92 mm** verification standards at 40 GHz

Verification	S11		S21		S12		S22	
Standard	ANG /Deg	UNC +/-	ANG /Deg	UNC +/-	ANG /Deg	UNC +/-	ANG /Deg	UNC +/-
50 Ω	-163.9	180.0	-7.06	8.90	-7.04	8.90	-6.81	180.0
20 dB	-37.94	11.34	-164.15	8.90	-164.29	8.90	70.87	10.74
50 dB	2.87	19.86	127.65	6.62	127.51	6.62	122.3	8.47
25 Ω	75.54	9.30	-17.35	8.90	-16.16	8.90	75.17	9.30

In addition, verifications with 3.5 mm standards have been performed using the 85053B Verification Kit (made by Agilent Technologies). The following tables (Table 3-3: magnitude data; Table 3-4: phase data) show the reported data of the 3.5 mm precision standards as delivered in the device characterization data sheet, for the 20 GHz frequency.

Table 3-3   Reported **magnitude** data and magnitude uncertainties of the **3.5 mm** precision verification standards at 20 GHz

Verification	S11		S21		S12		S22	
Standard	MAG lin	UNC +/-	MAG /dB	UNC +/-	MAG /dB	UNC +/-	MAG lin	UNC +/-
50 Ω	.00017	.00367	-.203	.015	-.202	.015	.00129	.00371
20 dB	.03096	.00214	-20.343	.019	-20.349	.019	.02080	.00234
40 dB	.04994	.00213	-40.433	.040	-40.444	.040	.03536	.00233
25 Ω	.49242	.00363	-1.511	.028	-1.518	.028	.49152	.00393

Table 3-4   Reported **phase** data and phase uncertainties of the **3.5 mm** precision verification standards at 20 GHz

Verification	S11		S21		S12		S22	
Standard	ANG /Deg	UNC +/-	ANG /Deg	UNC +/-	ANG /Deg	UNC +/-	ANG /Deg	UNC +/-
50 Ω	-35.06	180.0	-13.97	.93	-13.99	.93	-77.98	180.0
20 dB	27.65	4.16	-87.54	.97	-87.51	.97	-6.03	7.99
40 dB	49.26	2.65	-138.82	1.12	-138.40	1.12	44.04	5.31
25 Ω	-86.61	.62	-12.33	1.03	-12.40	1.03	-116.06	1.97

The complete evaluation procedure of the performed verification measurements has been divided into three phases described in detail in the following chapters:

4 Uncertainties of Transmission Measurements

Transmission Uncertainties for Matched DUTs

The first phase of the verification procedure was to determine the transmission uncertainties for matched DUTs as stated in the ZVK data sheet (PD 757.5543.22). The transmission coefficients (S_{21} and S_{12}) of each of the three matched verification standards, the 50 Ω airline and the two attenuators, were measured with the calibrated analyzer as a function of frequency. Additionally, both attenuators were cascaded and measured as a 70 dB device (60 dB for the 3.5 mm standards). All the obtained measurement results were compared with the reported data from the verification kit.

Theoretically, the forward (S_{21}) and reverse transmissions (S_{12}) of a reciprocal device, e.g. of an airline or an attenuator, are identical and should therefore result in identical measurement results from a well calibrated network analyzer. This is the case for the verification results obtained with the ZVK as can be seen in diagrams Fig. 4-1 to Fig. 4-16. The observed differences between the traces for S_{21} and S_{12} were in the order of a few hundreds of a dB for the magnitude and a few tenths of a degree for the phase.

The attenuation of the 50 Ω airline is only a few tenths of a dB higher than 0 dB. Due to the mechanical length of the 50 Ω airline, 75 mm, its transmission phase response can be described in a good approximation as:

φ = -360°·τ·f, with $\tau \approx$ 250 ps for an airline with length 75 mm.

The phase shift of the airline is linearly decreasing with increasing frequency, starting with 0° at DC and approaching approximately -3,600° for the highest frequency f = 40 GHz .

The attenuations of the verification attenuators correspond very well to their nominal values. The electrical delay of both 2.92 mm attenuators is roughly 90 ps which yields a phase shift of roughly -1,300° at 40 GHz.

The measurement accuracy for transmission measurements is shown in the diagrams Fig. 4-1 to Fig. 4-16. The transmission losses of the DUT were gradually increased starting with 0 dB up to 70 dB. The observed differences in magnitude and phase between the results of the verification measurements obtained with the ZVK and the measurement results reported by the manufacturer of the verification kit are displayed as blue (S_{21}) and green traces (S_{12}). (In black and white the green trace appears darker than the blue trace.) The uncertainties of the standards as reported by the manufacturers are illustrated as blue and green bars. The accuracy specifications of the ZVK are inserted as red crosses (+).
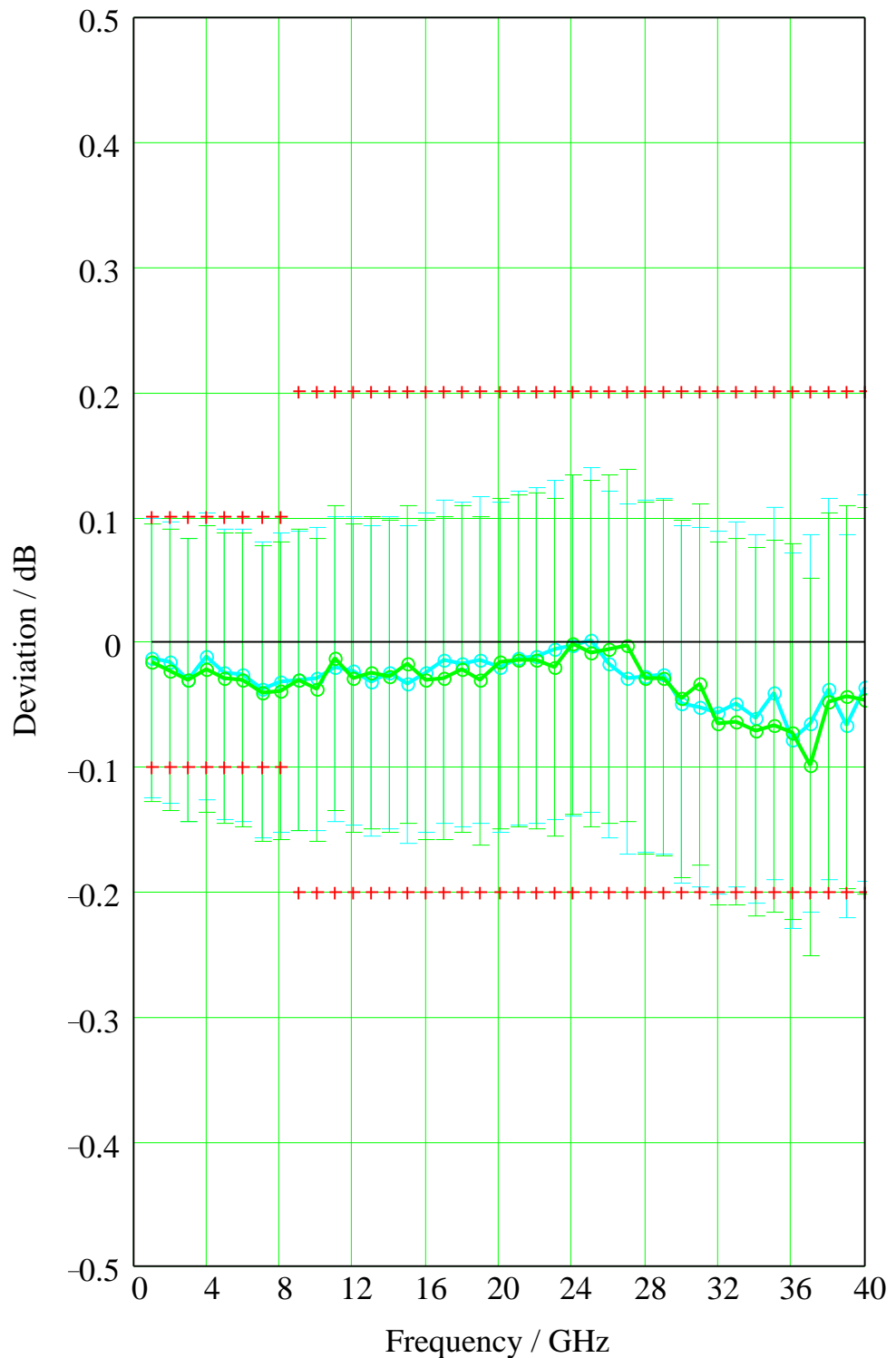
Fig. 4-1   Transmission **magnitude** deviations: **2.92 mm** 50 Ω airline verification standard at **0 dB**

The magnitude difference (blue trace S_{21} and green trace S_{12}) between the results obtained by verification measurements with a ZVK and the data for the verification standard reported by the manufacturer. Additionally, the reported uncertainties for the verification standard (blue and green bars) and the accuracy specifications of the ZVK (red crosses) are displayed.
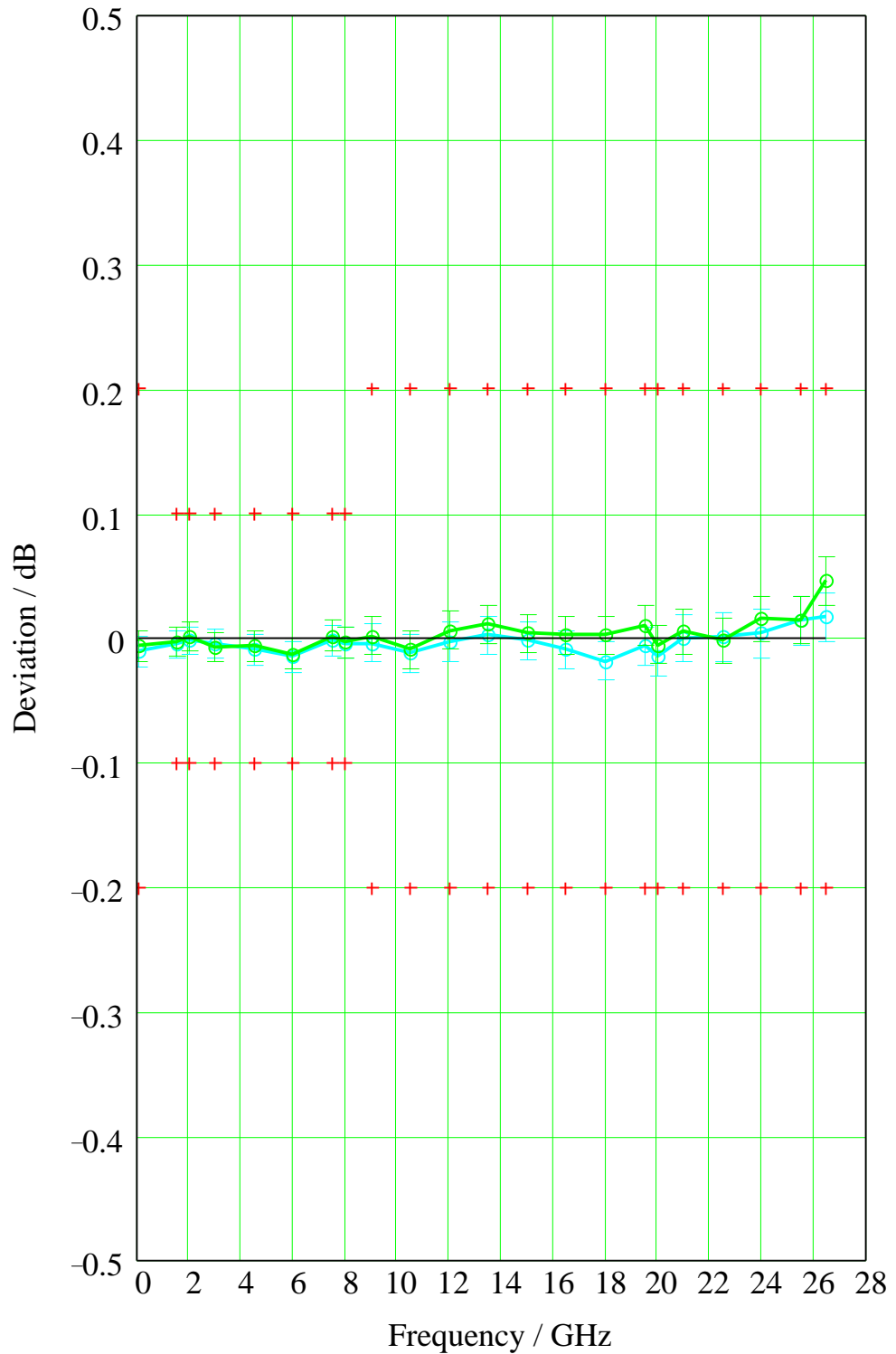
Fig. 4-2   Transmission **phase** deviations: **2.92 mm** 50 Ω airline verification standard at **0 dB**

The phase difference (blue trace S_{21} and green trace S_{12}) between the results obtained by verification measurements with a ZVK and the reported measurement data for the verification standard. Additionally, the reported uncertainties for the verification standard (blue and green bars) and the accuracy specifications of the ZVK (red crosses) are displayed.
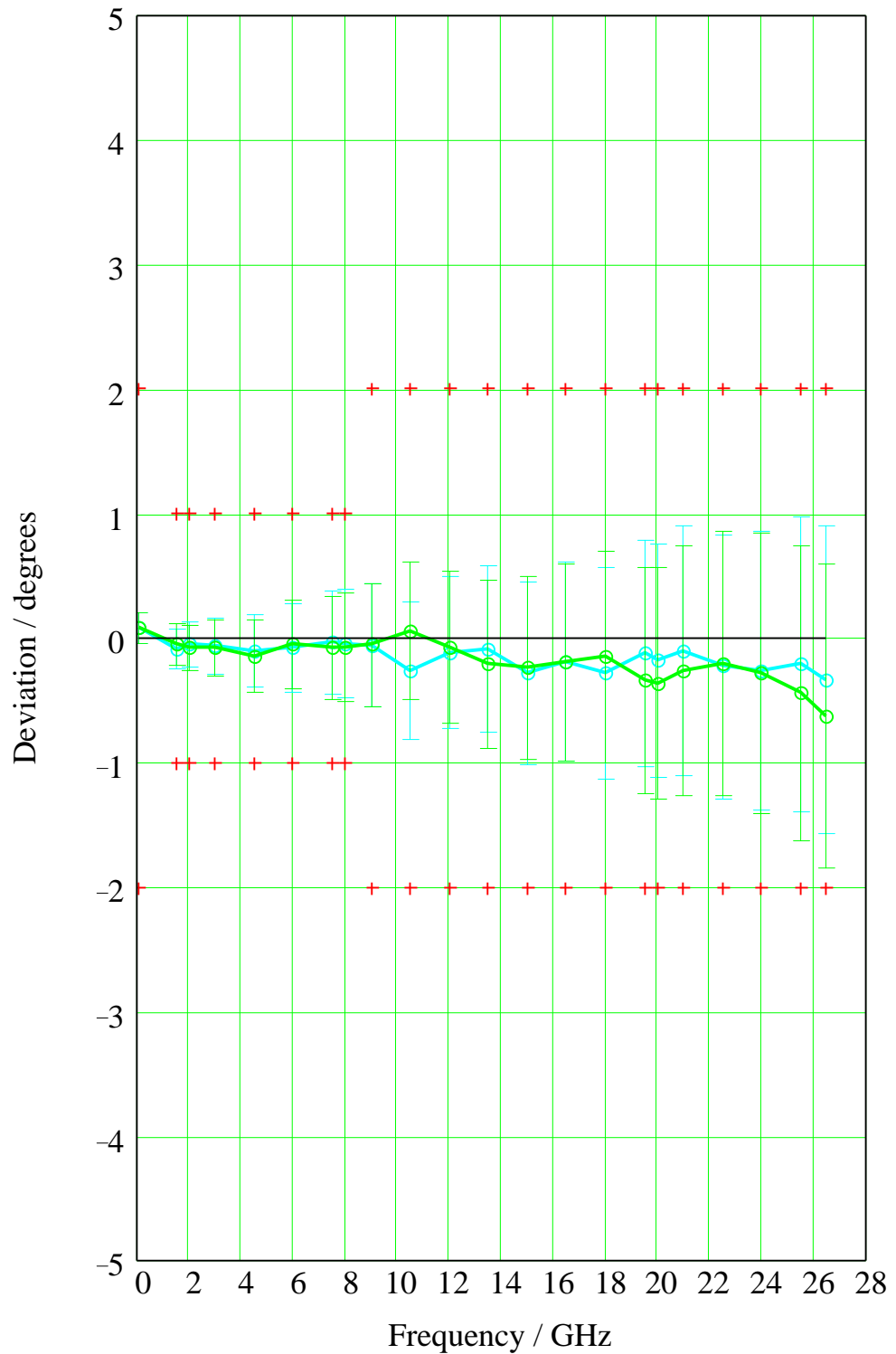
Fig. 4-3   Transmission **magnitude** deviations: **3.5 mm** 50 Ω airline verification standard at **0 dB**

The magnitude difference (blue trace S_{21} and green trace S_{12}) between the results obtained by verification measurements with a ZVK and the data for the verification standard reported by the manufacturer. Additionally, the reported uncertainties for the verification standard (blue and green bars) and the accuracy specifications of the ZVK (red crosses) are displayed.
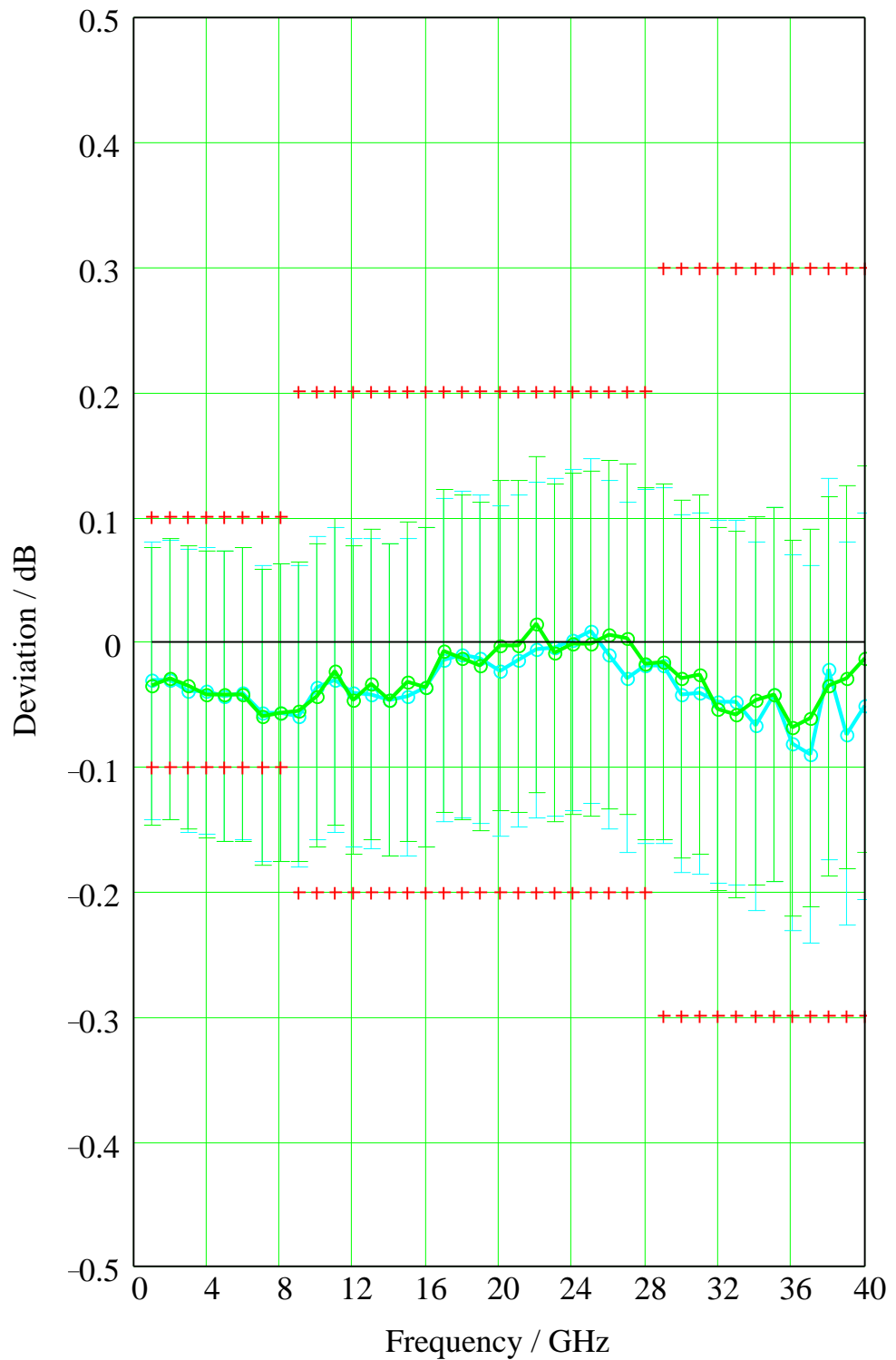
Fig. 4-4   Transmission **phase** deviations: **3.5 mm** 50 Ω airline verification standard at **0 dB**

The phase difference (blue trace S_{21} and green trace S_{12}) between the results obtained by verification measurements with a ZVK and the reported measurement data for the verification standard. Additionally, the reported uncertainties for the verification standard (blue and green bars) and the accuracy specifications of the ZVK (red crosses) are displayed.
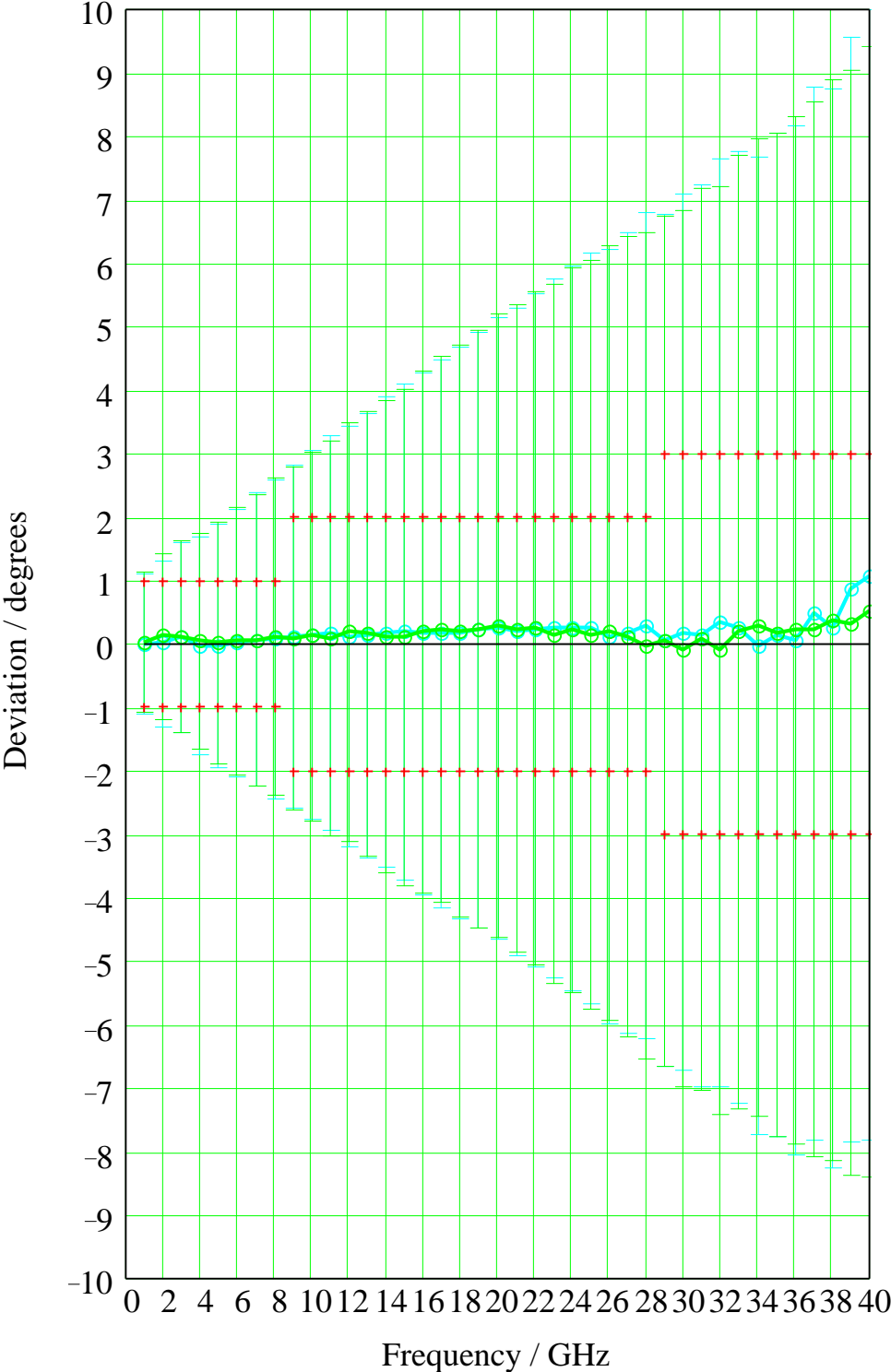
Fig. 4-5   Transmission **magnitude** deviations: **2.92 mm 20 dB** attenuation standard

The magnitude difference (blue trace S_{21} and green trace S_{12}) between the results obtained by verification measurements with a ZVK and the data for the verification standard reported by the manufacturer. Additionally, the reported uncertainties for the verification standard (blue and green bars) and the accuracy specifications of the ZVK (red crosses) are displayed.

Fig. 4-6   Transmission **phase** deviations: **2.92 mm 20 dB** attenuation standard

The phase difference (blue trace S_{21} and green trace S_{12}) between the results obtained by verification measurements with a ZVK and the reported measurement data for the verification standard. Additionally, the reported uncertainties for the verification standard (blue and green bars) and the accuracy specifications of the ZVK (red crosses) are displayed.
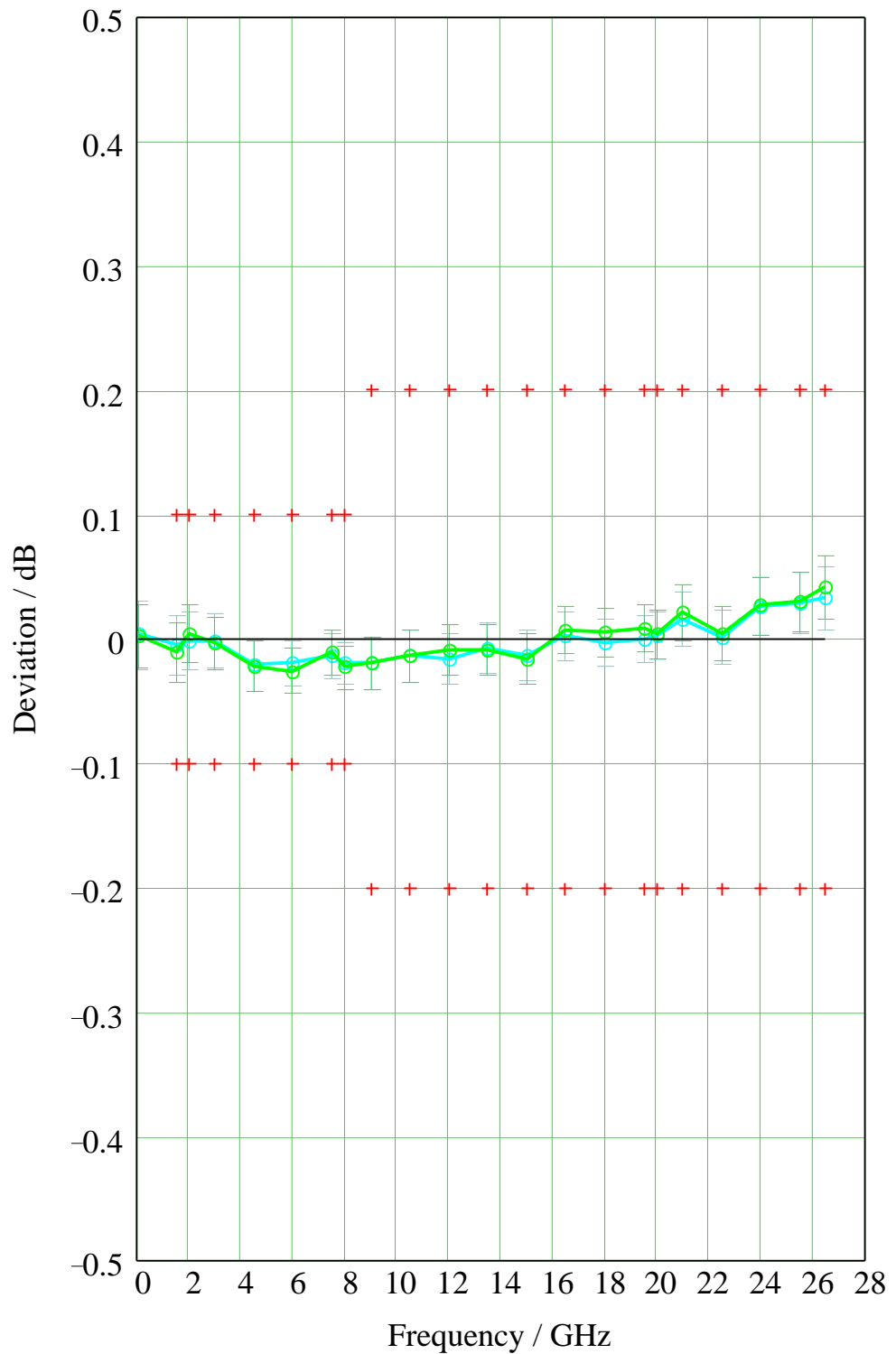
Fig. 4-7   Transmission **magnitude** deviations: **3.5 mm 20 dB** attenuation standard

The magnitude difference (blue trace S_{21} and green trace S_{12}) between the results obtained by verification measurements with a ZVK and the data for the verification standard reported by the manufacturer. Additionally, the reported uncertainties for the verification standard (blue and green bars) and the accuracy specifications of the ZVK (red crosses) are displayed.
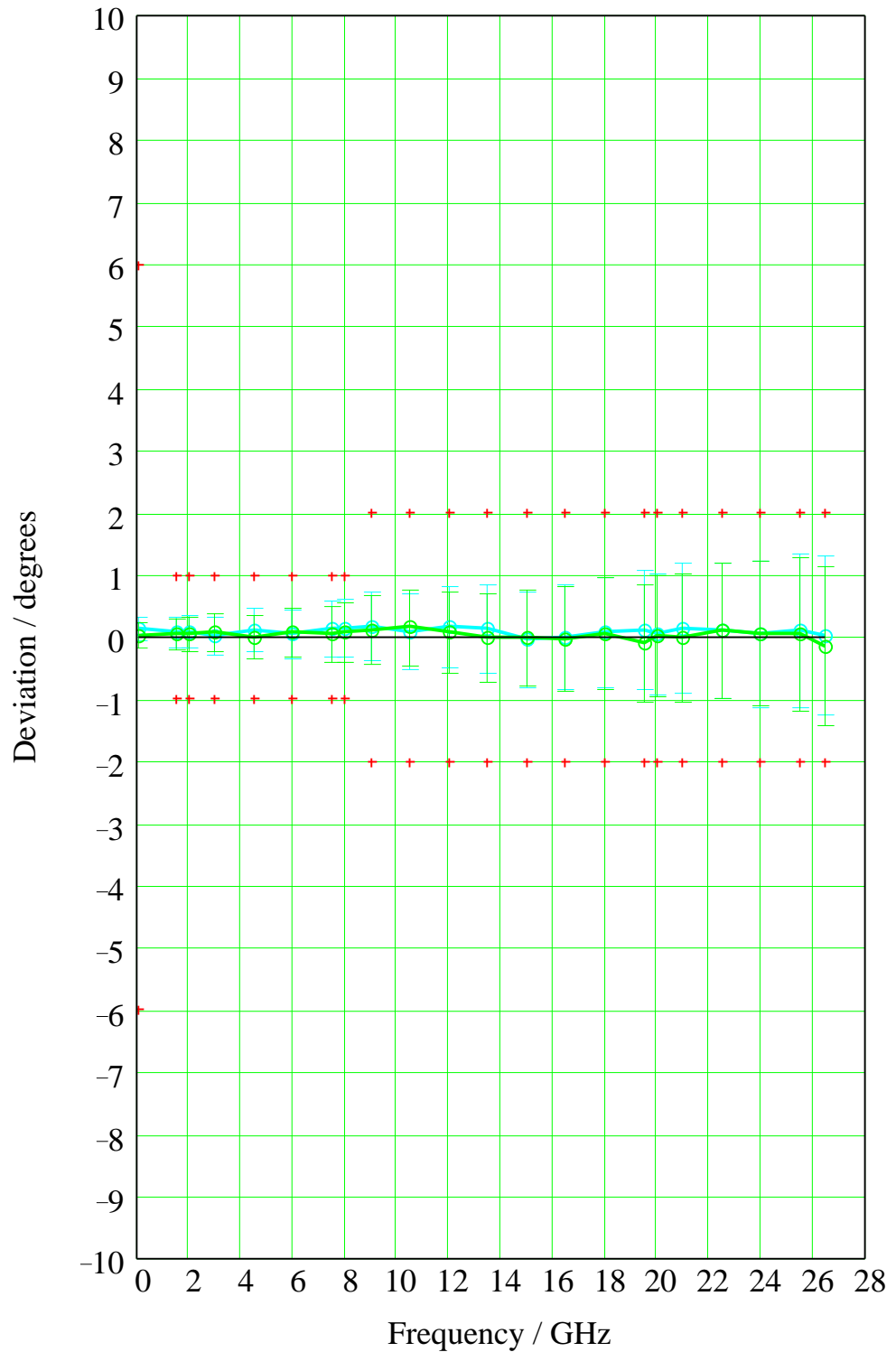
Fig. 4-8   Transmission **phase** deviations: **3.5 mm 20 dB** attenuation standard

The phase difference (blue trace S_{21} and green trace S_{12}) between the results obtained by verification measurements with a ZVK and the reported measurement data for the verification standard. Additionally, the reported uncertainties for the verification standard (blue and green bars) and the accuracy specifications of the ZVK (red crosses) are displayed.
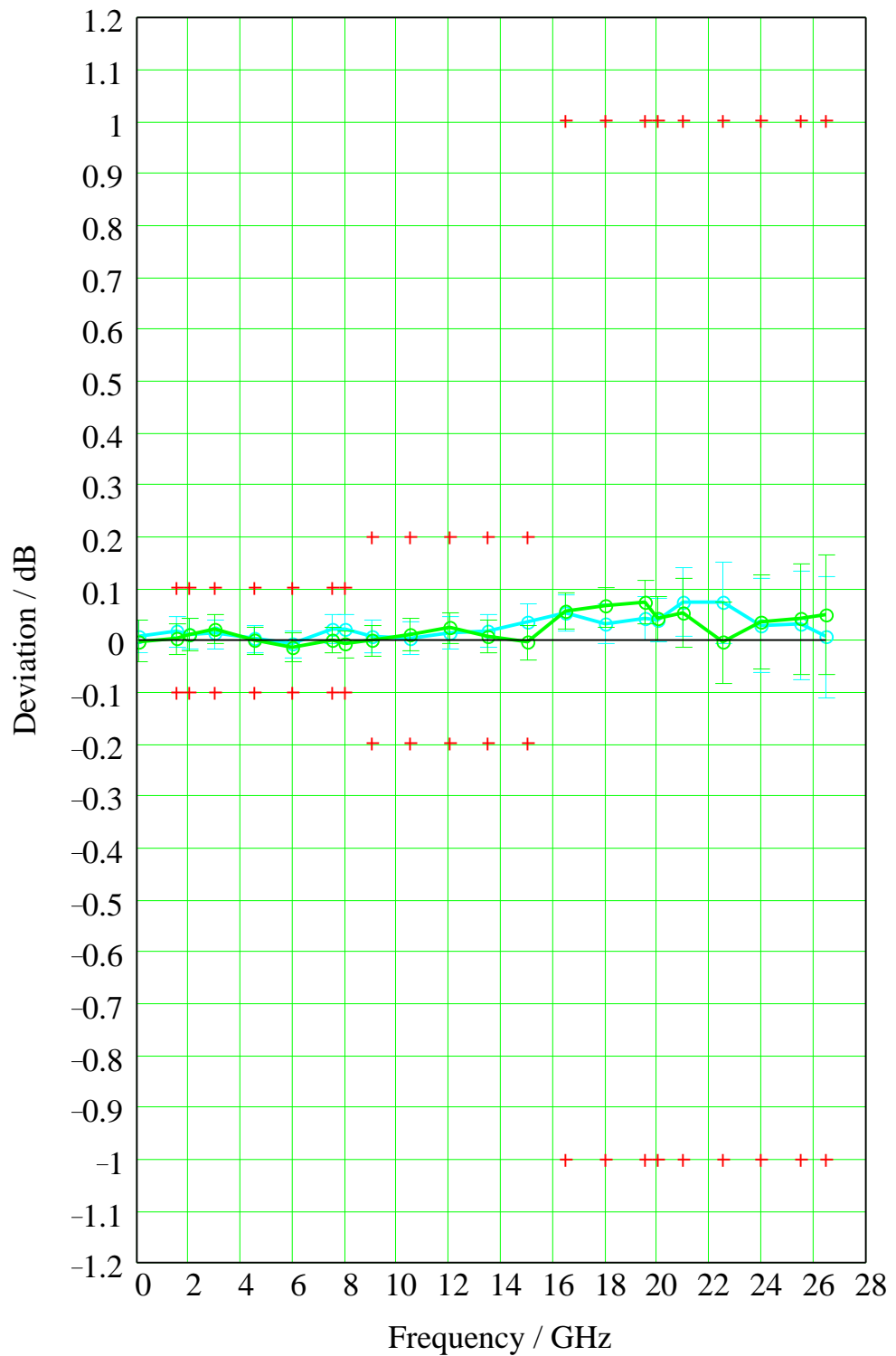
Fig. 4-9   Transmission **magnitude** deviations: **3.5 mm 40 dB** attenuation standard

The magnitude difference (blue trace S_{21} and green trace S_{12}) between the results obtained by verification measurements with a ZVK and the data for the verification standard reported by the manufacturer. Additionally, the reported uncertainties for the verification standard (blue and green bars) and the accuracy specifications of the ZVK (red crosses) are displayed.
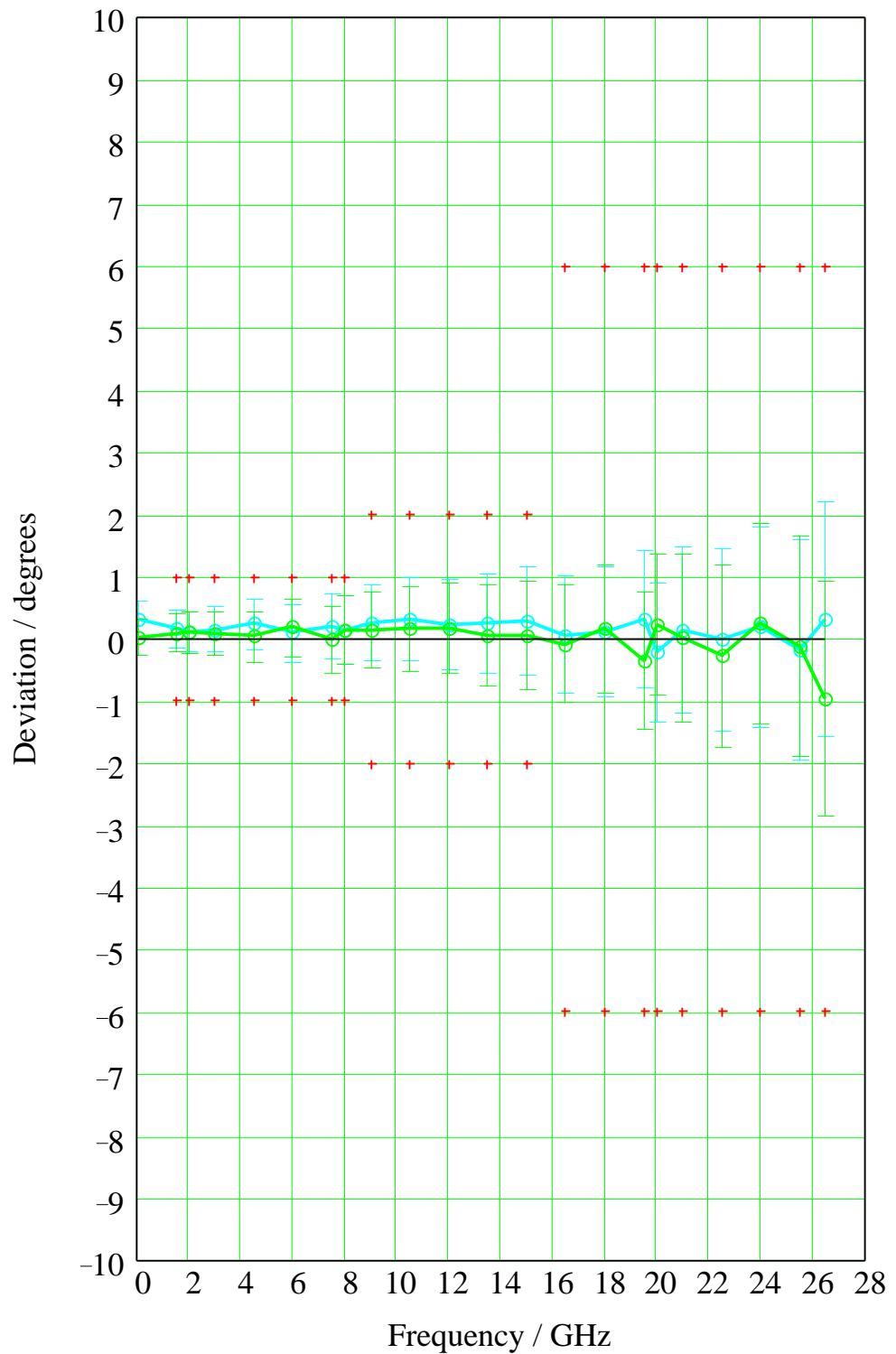
Fig. 4-10   Transmission **phase** deviations: **3.5 mm 40 dB** attenuation standard

The phase difference (blue trace S_{21} and green trace S_{12}) between the results obtained by verification measurements with a ZVK and the reported measurement data for the verification standard. Additionally, the reported uncertainties for the verification standard (blue and green bars) and the accuracy specifications of the ZVK (red crosses) are displayed.

Fig. 4-11   Transmission **magnitude** deviations: **2.92 mm 50 dB** attenuation standard

The magnitude difference (blue trace S_{21} and green trace S_{12}) between the results obtained by verification measurements with a ZVK and the data for the verification standard reported by the manufacturer. Additionally, the reported uncertainties for the verification standard (blue and green bars) and the accuracy specifications of the ZVK (red crosses) are displayed.
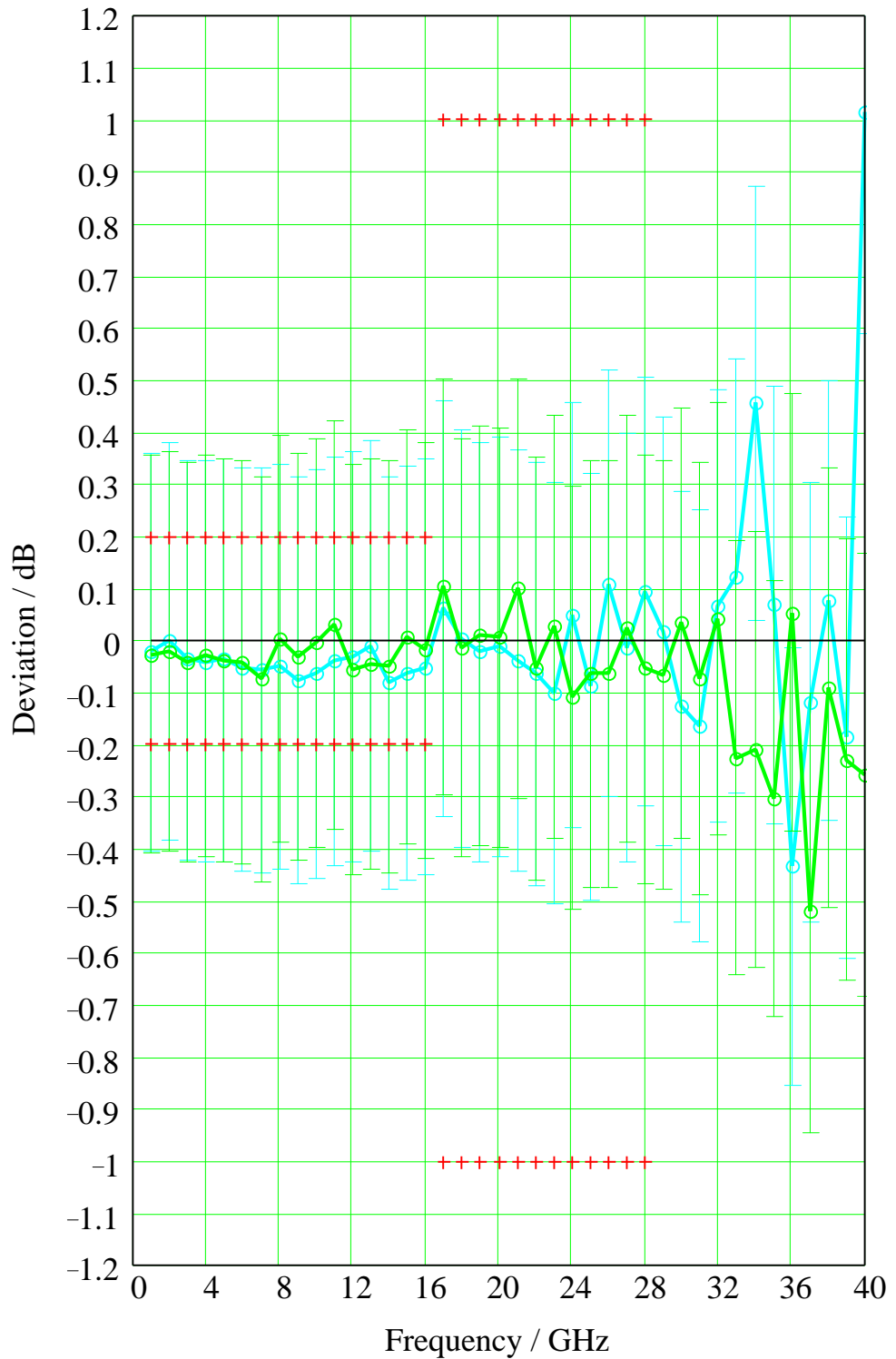
Fig. 4-12   Transmission **phase** deviations: **2.92 mm 50 dB** attenuation standard

The phase difference (blue trace S_{21} and green trace S_{12}) between the results obtained by verification measurements with a ZVK and the reported measurement data for the verification standard. Additionally, the reported uncertainties for the verification standard (blue and green bars) and the accuracy specifications of the ZVK (red crosses) are displayed.
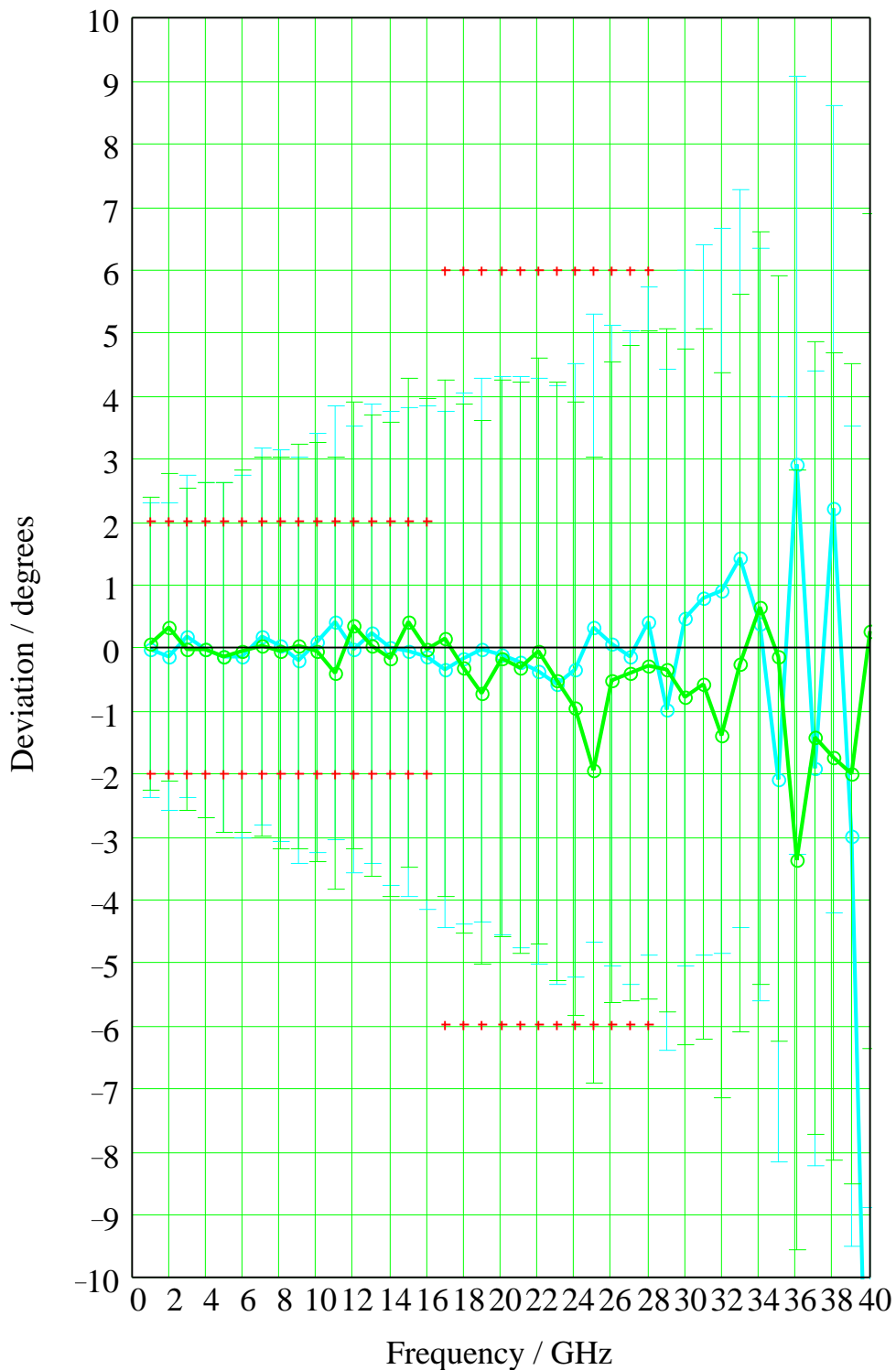
Fig. 4-13   Transmission **magnitude** deviations: **3.5 mm 60 dB** attenuation standard

The magnitude difference (blue trace S_{21} and green trace S_{12}) between the results obtained by verification measurements with a ZVK (cascaded 20 dB and 40 dB standards) and the data for the verification standards reported by the manufacturer. Additionally, the sum of the reported uncertainties for the verification standards (blue and green bars) and the accuracy specifications of the ZVK (red crosses) are displayed.
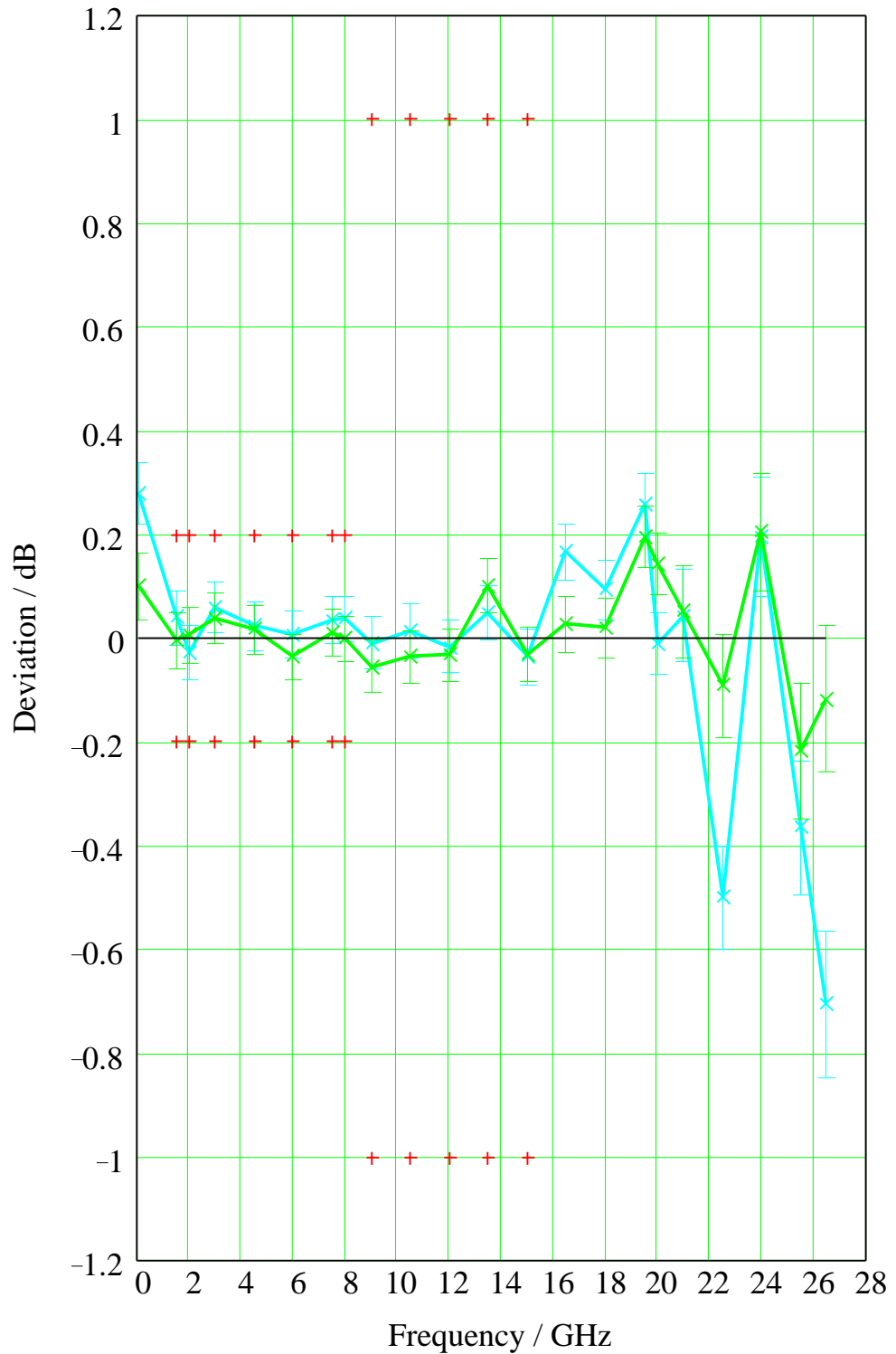
Fig. 4-14   Transmission **phase** deviations: **3.5 mm 60 dB** attenuation standard

The phase difference (blue trace S_{21} and green trace S_{12}) between the results obtained by verification measurements with a ZVK (cascaded 20 dB and 40 dB standards) and the data for the verification standards reported by the manufacturer. Additionally, the sum of the reported uncertainties for the verification standards (blue and green bars) and the accuracy specifications of the ZVK (red crosses) are displayed.
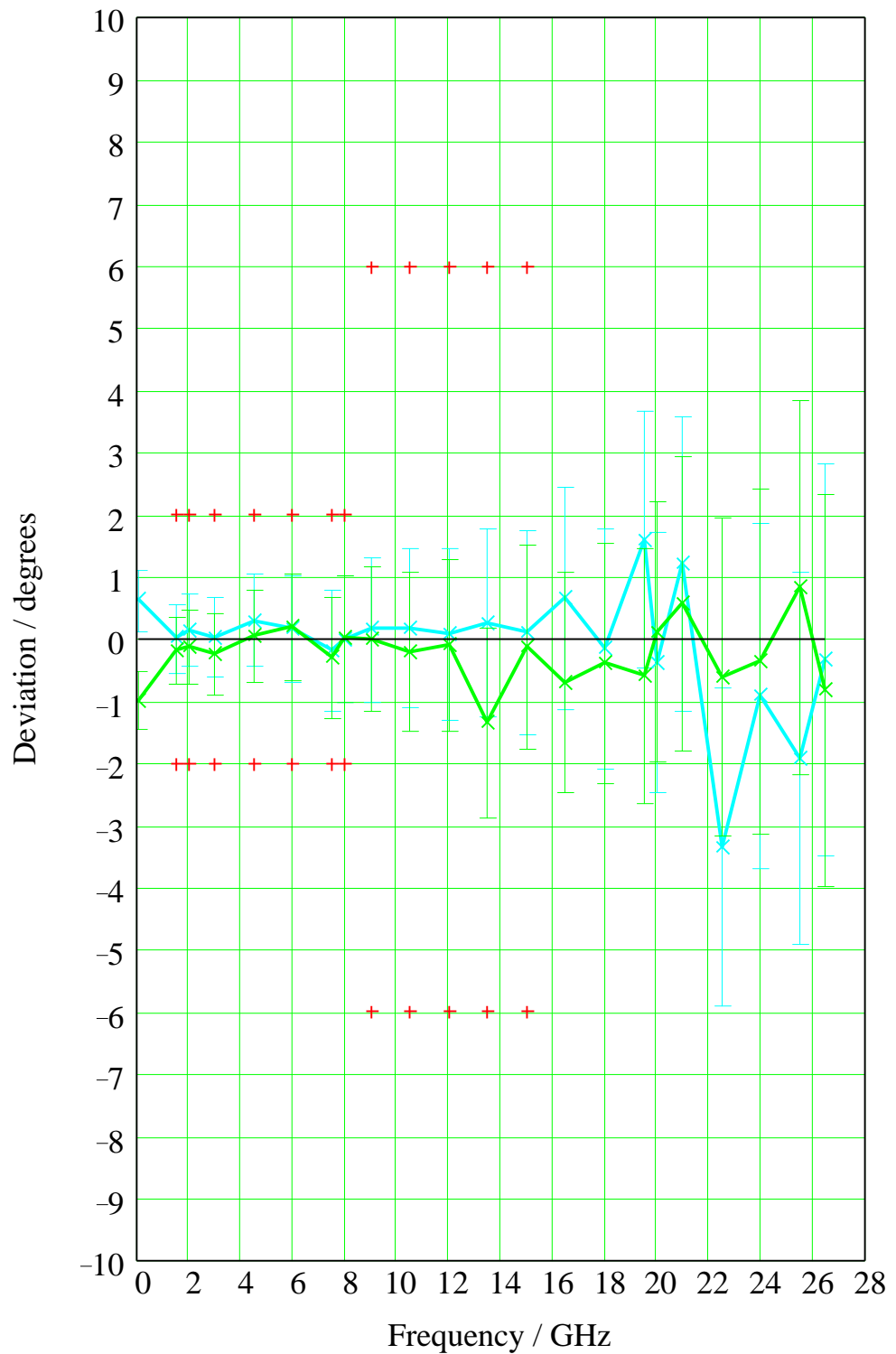
Fig. 4-15   Transmission **magnitude** deviations: **2.92 mm 70 dB** attenuation standard

The magnitude difference (blue trace S_{21} and green trace S_{12}) between the results obtained by verification measurements with a ZVK (cascaded 20 dB and 50 dB standards) and the data for the verification standards reported by the manufacturer. Additionally, the sum of the reported uncertainties for the verification standards (blue and green bars) and the accuracy specifications of the ZVK (red crosses) are displayed.
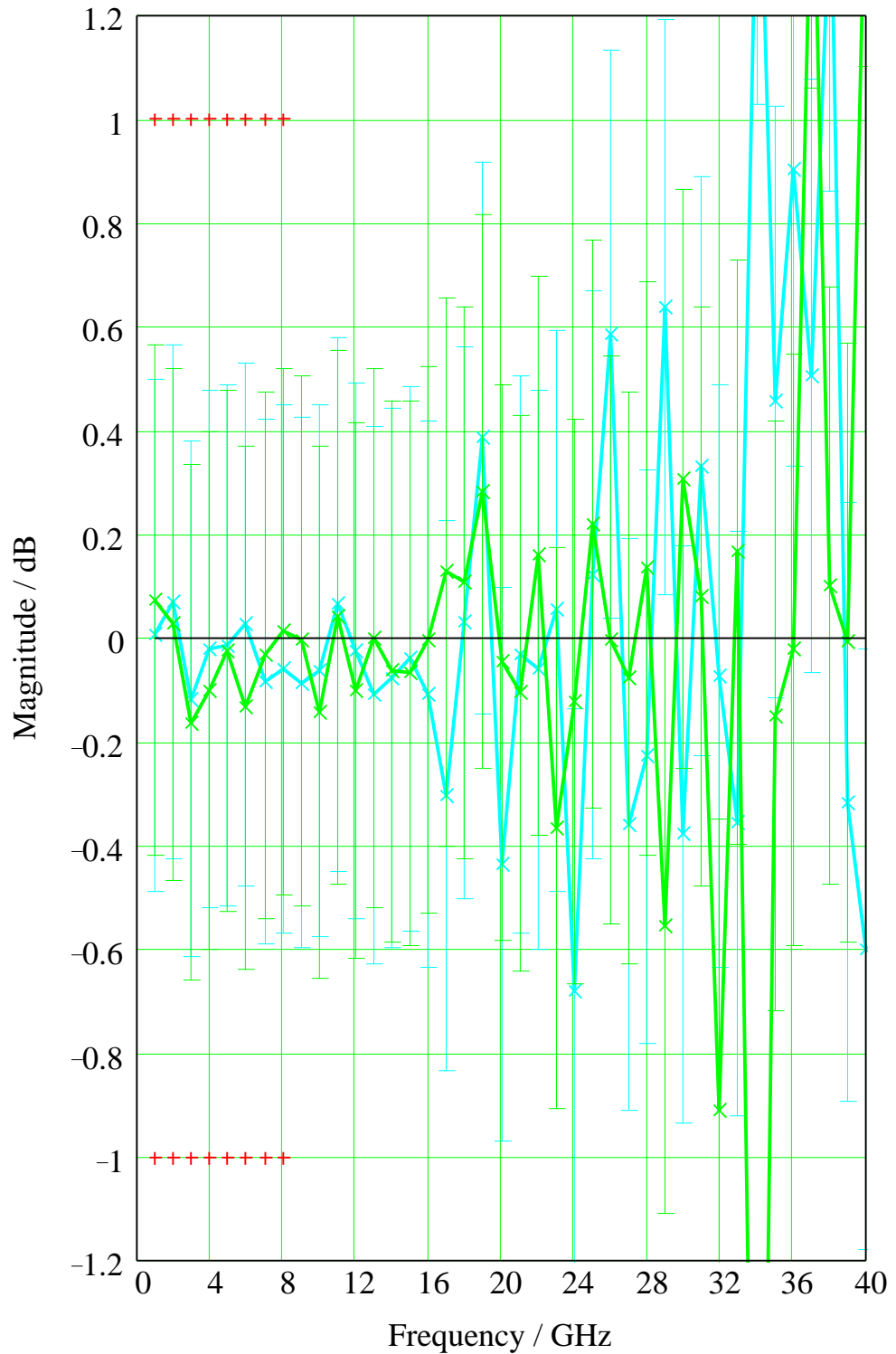
Fig. 4-16   Transmission **phase** deviations: **2.92 mm 70 dB** attenuation standard

The phase difference (blue trace S_{21} and green trace S_{12}) between the results obtained by verification measurements with a ZVK (cascaded 20 dB and 50 dB standards) and the data for the verification standards reported by the manufacturer. Additionally, the sum of the reported uncertainties for the verification standards (blue and green bars) and the accuracy specifications of the ZVK (red crosses) are displayed.
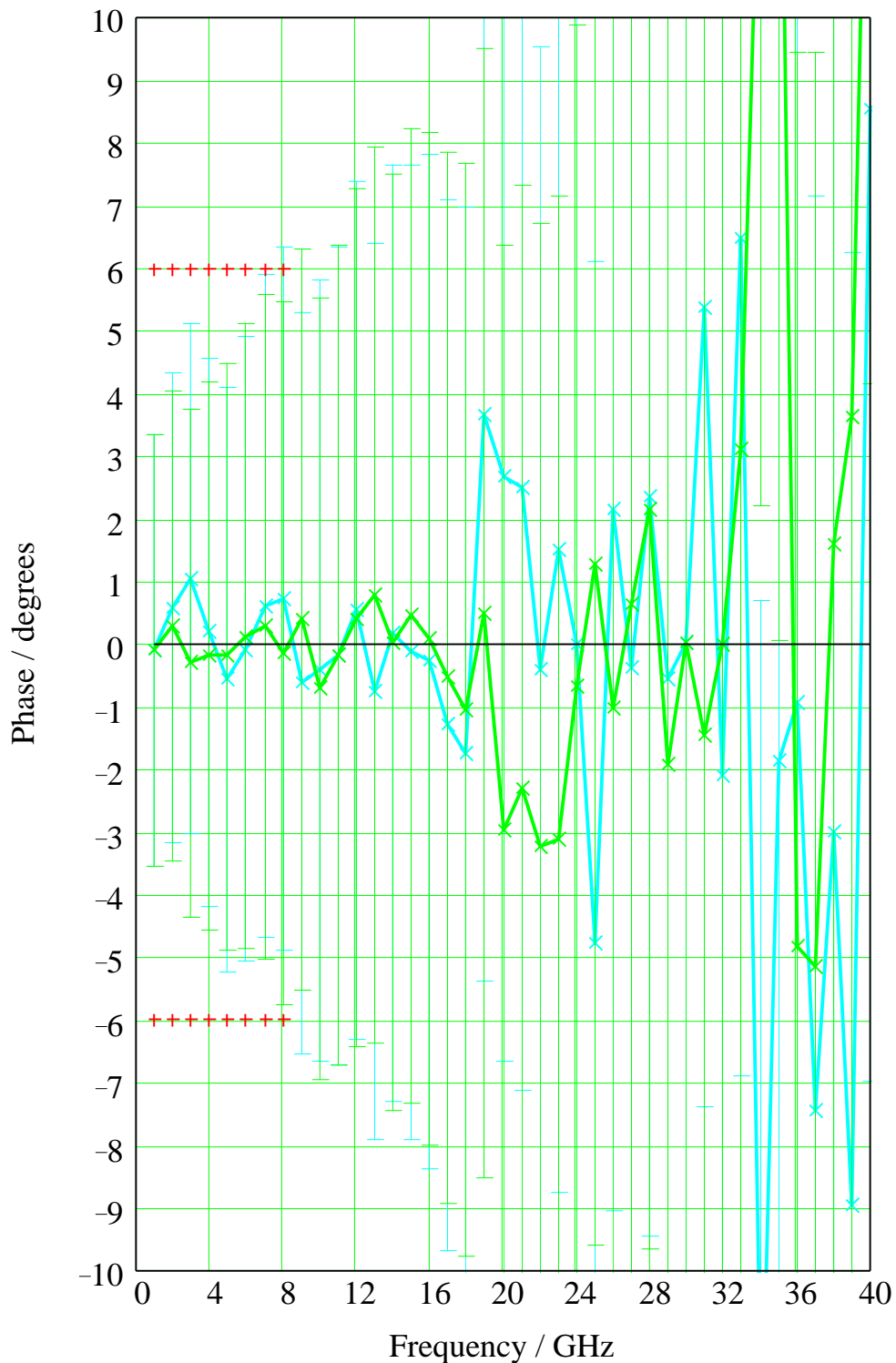
Transmission Uncertainties for a Mismatched DUT

Although transmission measurement accuracy is only specified for matched DUTs in the ZVK data sheet, transmission uncertainties should be additionally checked for a mismatched DUT due to its practical relevance. The transmission coefficients of the stepped airline verification standard (see Fig. 4-17) were measured.
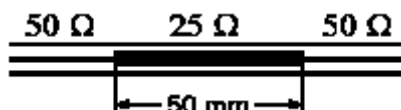

Fig. 4-17   Stepped airline (Beatty standard)

A Beatty airline provides an impedance step from 50 Ω to 25 Ω and back. It realizes a quarter-wavelength transformation at all odd integer multiples of the frequency f_o with $f_o = c / (4 \cdot L)$ where c is the velocity of light and L is the length of the 25 Ω section of the Beatty standard (L = 50 mm). At these particular frequencies, the standard is reflective comparable to an impedance of 12.5 Ω. Neglecting losses, $|r| = 60$ % or approx. -4.44 dB can be calculated. Consequently, the transmission coefficient is less than 0 dB at these frequencies (for a lossless standard approx. -1.94 dB). At all integer multiples of the frequency $2 \cdot f_o \approx 3$ GHz, the standard represents a half-wavelength transformation. It is well matched at these frequencies, and its transmission coefficient is theoretically 0 dB for a lossless standard. In practice, losses of a few tenths of a dB occur due to the finite conductivity of the conductors. Fig. 4-18 shows some simulation results for the magnitude of the transmission and the reflection of a stepped airline.
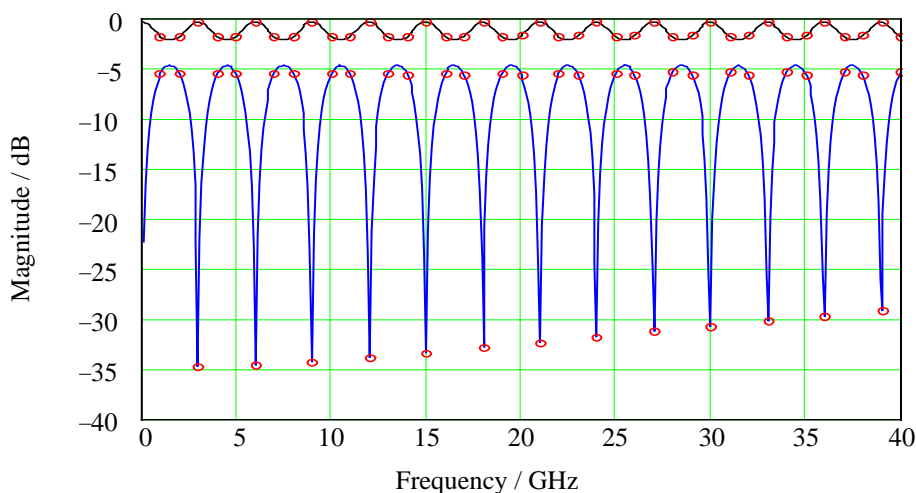

Fig. 4-18   Simulated magnitude response of a stepped airline

                       Transmission (upper trace) and reflection (lower trace). Red points indicate integer multiples of 1 GHz.

Fig. 4-19 to Fig. 4-22 (see pp. 23 - 26) present the results of the transmission verification measurements of the stepped airlines. The accuracy of transmission measurements is not specified in the ZVK data sheet for mismatched DUTs. Nevertheless, the verification results demonstrate that the deviation for transmission measurements of the (mismatched) stepped airlines is less than the specified uncertainties for matched DUTs. This proves to be correct, even at all odd integer multiples of the frequency $f_o \approx 1.5$ GHz at which the reflection coefficient of the standard is rather high (approximately 60 % corresponding to 4.44 dB return loss).

Fig. 4-19   Transmission **magnitude** deviations: **2.92 mm** stepped airline verification standard

The magnitude difference (blue trace S_{21} and green trace S_{12}) between the results obtained by verification measurements with a ZVK and the data for the verification standard reported by the manufacturer. Additionally, the reported uncertainties for the verification standard (blue and green bars) and the accuracy specifications of the ZVK (red crosses) are displayed. The accuracy of transmission measurements for mismatched DUTs is **not specified** in the ZVK data sheet. For information only, the ZVK specifications for matched DUTs are inserted (blue crosses).

Fig. 4-20   Transmission **phase** deviations: **2.92 mm** stepped airline verification standard

The phase difference (blue trace S_{21} and green trace S_{12}) between the results obtained by verification measurements with a ZVK and the data for the verification standard reported by the manufacturer. Additionally, the reported uncertainties for the verification standard (blue and green bars) and the accuracy specifications of the ZVK (red crosses) are displayed. The accuracy of transmission measurements for mismatched DUTs is **not specified** in the ZVK data sheet. For information only, the ZVK specifications for matched DUTs are inserted (blue crosses).
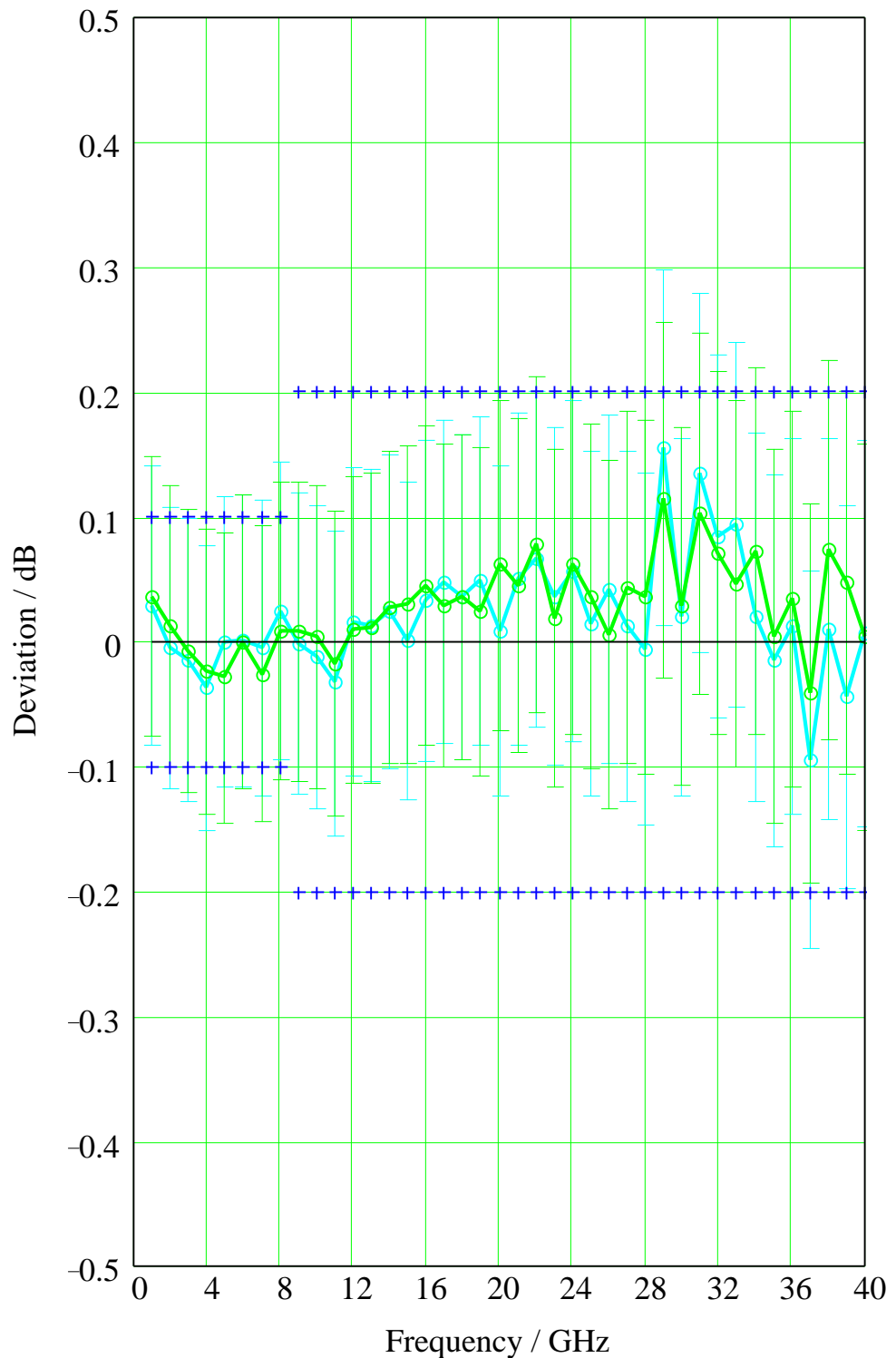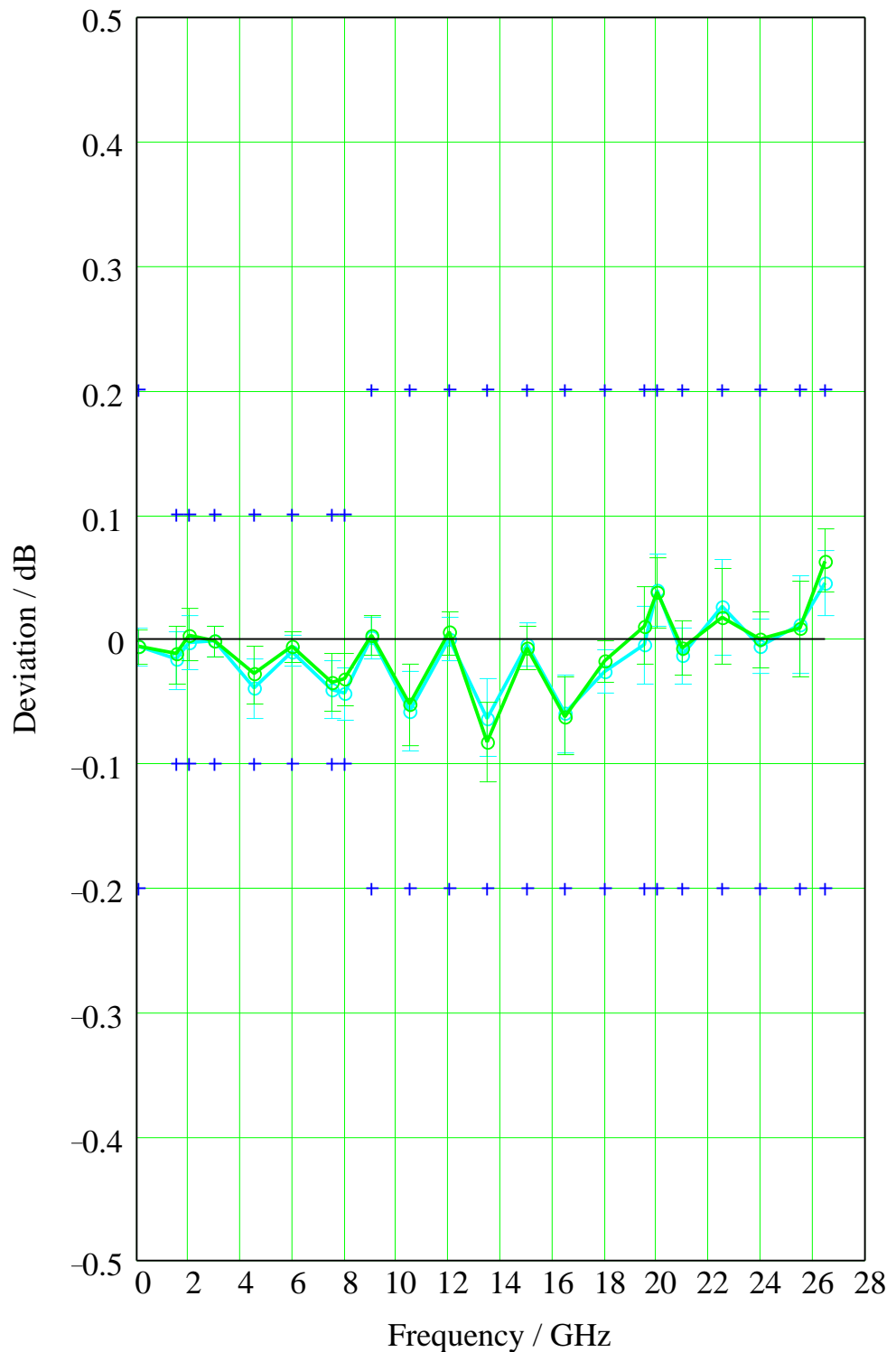
Fig. 4-21   Transmission **magnitude** deviations: **3.5 mm** stepped airline verification standard

The magnitude difference (blue trace S_{21} and green trace S_{12}) between the results obtained by verification measurements with a ZVK and the data for the verification standard reported by the manufacturer. Additionally, the reported uncertainties for the verification standard (blue and green bars) and the accuracy specifications of the ZVK (red crosses) are displayed. The accuracy of transmission measurements for mismatched DUTs is **not specified** in the ZVK data sheet. For information only, the ZVK specifications for matched DUTs are inserted (blue crosses).
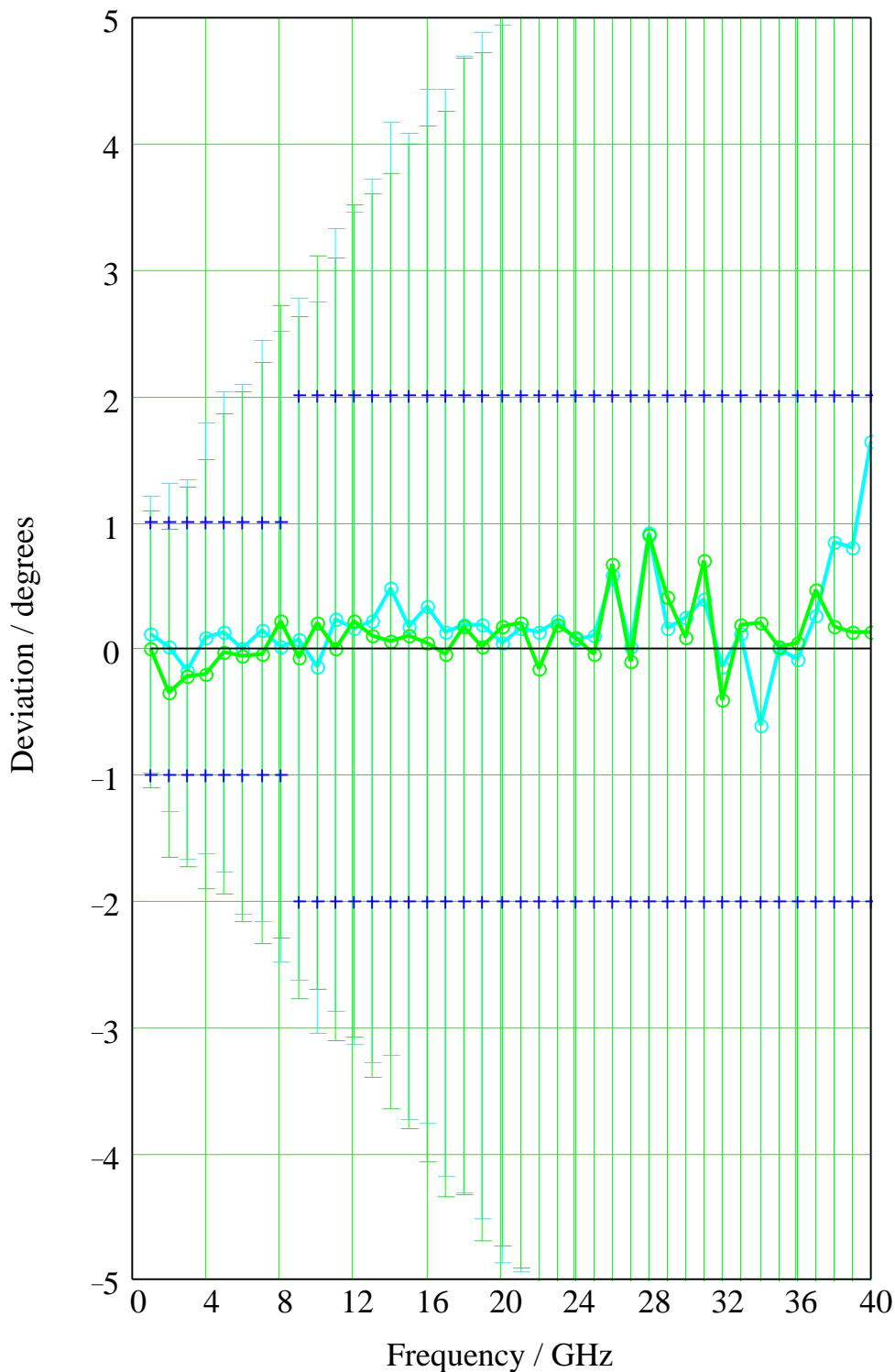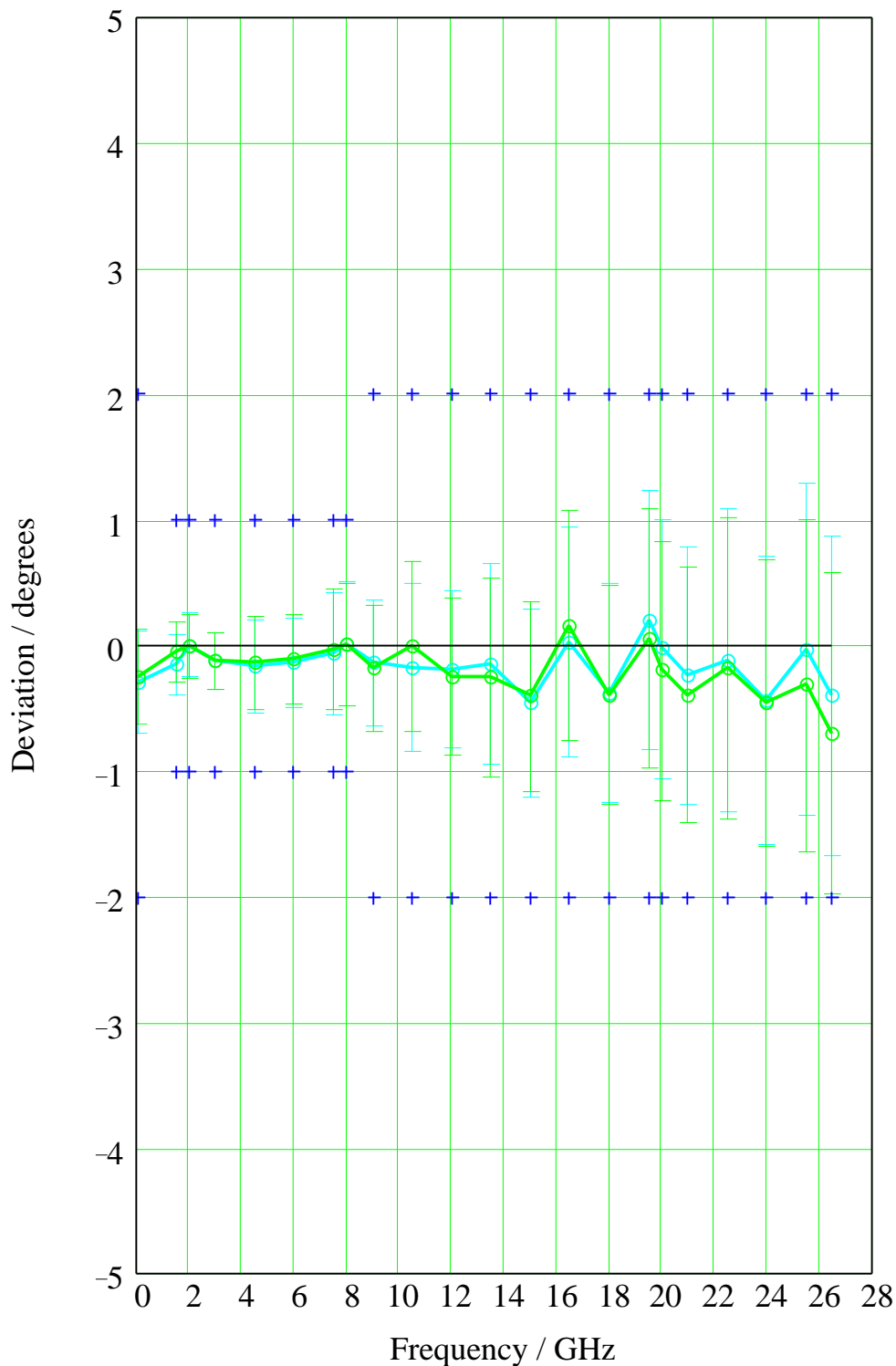
Fig. 4-22　　　　Transmission **phase** deviations: **3.5 mm** stepped airline verification standard

The phase difference (blue trace S_{21} and green trace S_{12}) between the results obtained by verification measurements with a ZVK and the data for the verification standard reported by the manufacturer. Additionally, the reported uncertainties for the verification standard (blue and green bars) and the accuracy specifications of the ZVK (red crosses) are displayed. The accuracy of transmission measurements for mismatched DUTs is **not specified** in the ZVK data sheet. For information only, the ZVK specifications for matched DUTs are inserted (blue crosses).

5 Uncertainties of Reflection Measurements

The second phase of the verification for the ZVK was to determine the reflection uncertainties of the network analyzer (see ZVK data sheet PD 757.5543.22). Unfortunately, no precise one-port reflection standards with well defined reflection coefficients are available which would be useful for a direct check of reflection measurement accuracy.

An important exception is the SHORT standard. It is a one-port standard with a well defined reflection coefficient. The magnitude of the reflection coefficient of the calibration standard SHORT can be assumed to be precisely 0 dB at all frequencies - under the assumption that its electrical length is small and its losses are negligible. After subtracting the phase shift caused by the electrical length of the standard, its reflection coefficient can in good approximation be assumed as r = -1. So, a precise SHORT standard is a nearly ideal standard for the verification of the measurement accuracy for high reflection coefficients.

This is only true, if the SHORT is not applied as a calibration standard during a TOSM-calibration. The re-use of the standard in order to attempt a verification would only yield a criterion for the repeatability of the measurement and the stability of the system. But it would *not* provide the required indication for the measurement accuracy. It would simply be a re-identification of the calibration standard and no real verification as desired.

As stated in chapter 2 (see page 3), the R&S patented method TOM was chosen to calibrate the ZVK. It is one of the more sophisticated calibration techniques, offered for the ZVK along with TRM, TNA (both R&S patents, too) and TRL. These techniques require a two-port network analyzer with four receiver channels (ZVR, ZVC, ZVM, or ZVK). Analyzers with only three receiver channels (e.g. ZVRE) are not sufficient for these calibration techniques.

One advantage of the TOM method is that the SHORT calibration standard is not needed for the calibration procedure. Therefore, it is still fully available as a *verification* standard after calibration. Hence, a simple connection of the SHORT standards to the reference planes of PORT 1 and PORT 2 after performing a TOM calibration will result in a direct verification of the measurement accuracy of the network analyzer for reflection measurements at r = -1 (0 dB). The verification results of the magnitudes and phases are presented in Fig. 5-1 and Fig. 5-2. For the phase display, the known electrical lengths of the SHORT standards were subtracted and an additional phase offset of 180° was used.

Figures 5-3 to 5-5 show the results of the reflection verification measurements using the stepped airline standard.
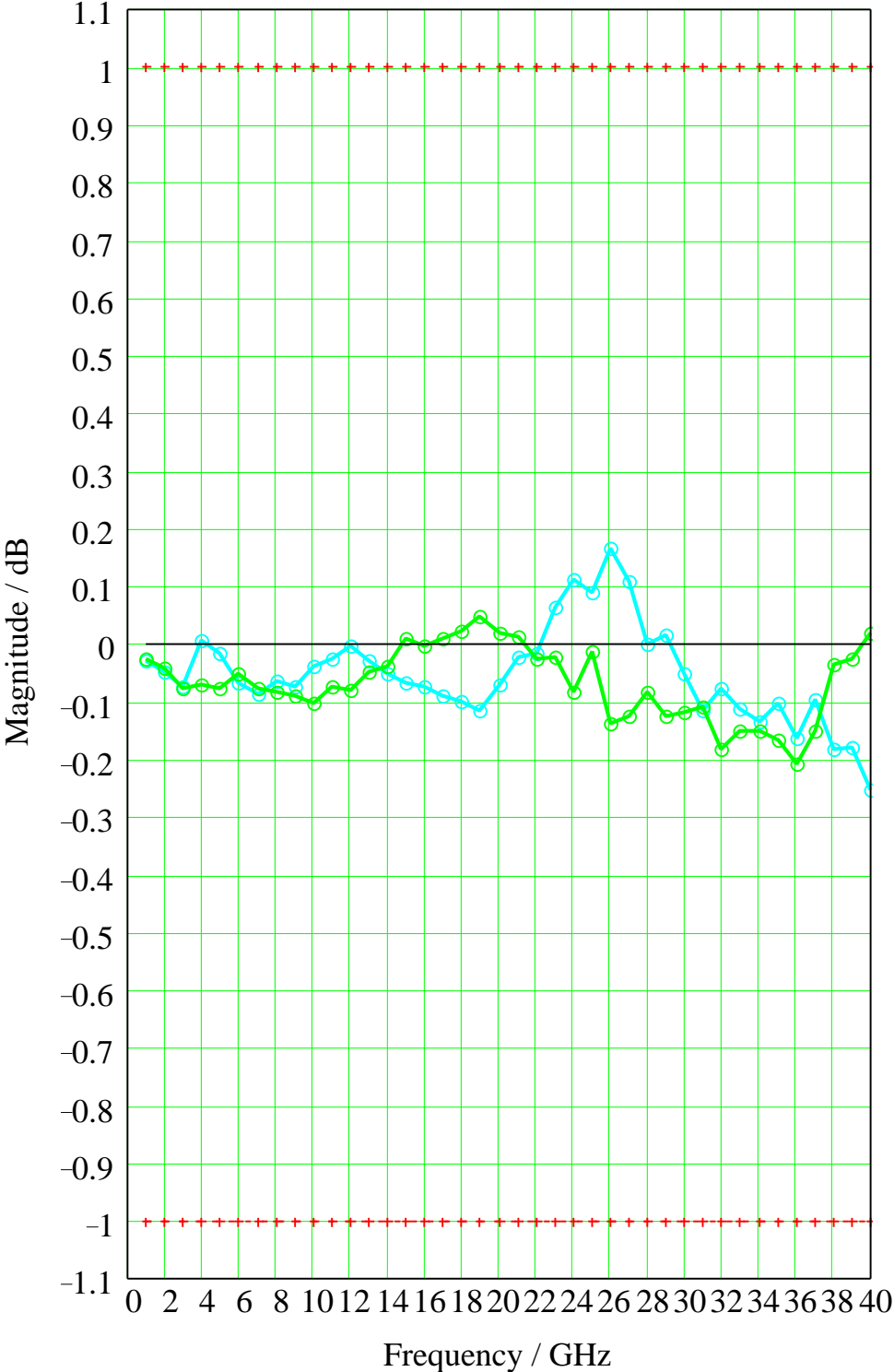
Fig. 5-1   Reflection **magnitude** deviations: 2.92 mm SHORT verification standard (0 dB)

Verification measurement results of the SHORT standard (blue trace S_{11} and green trace S_{22}). Additionally, the accuracy specifications of the ZVK (red crosses) are displayed.
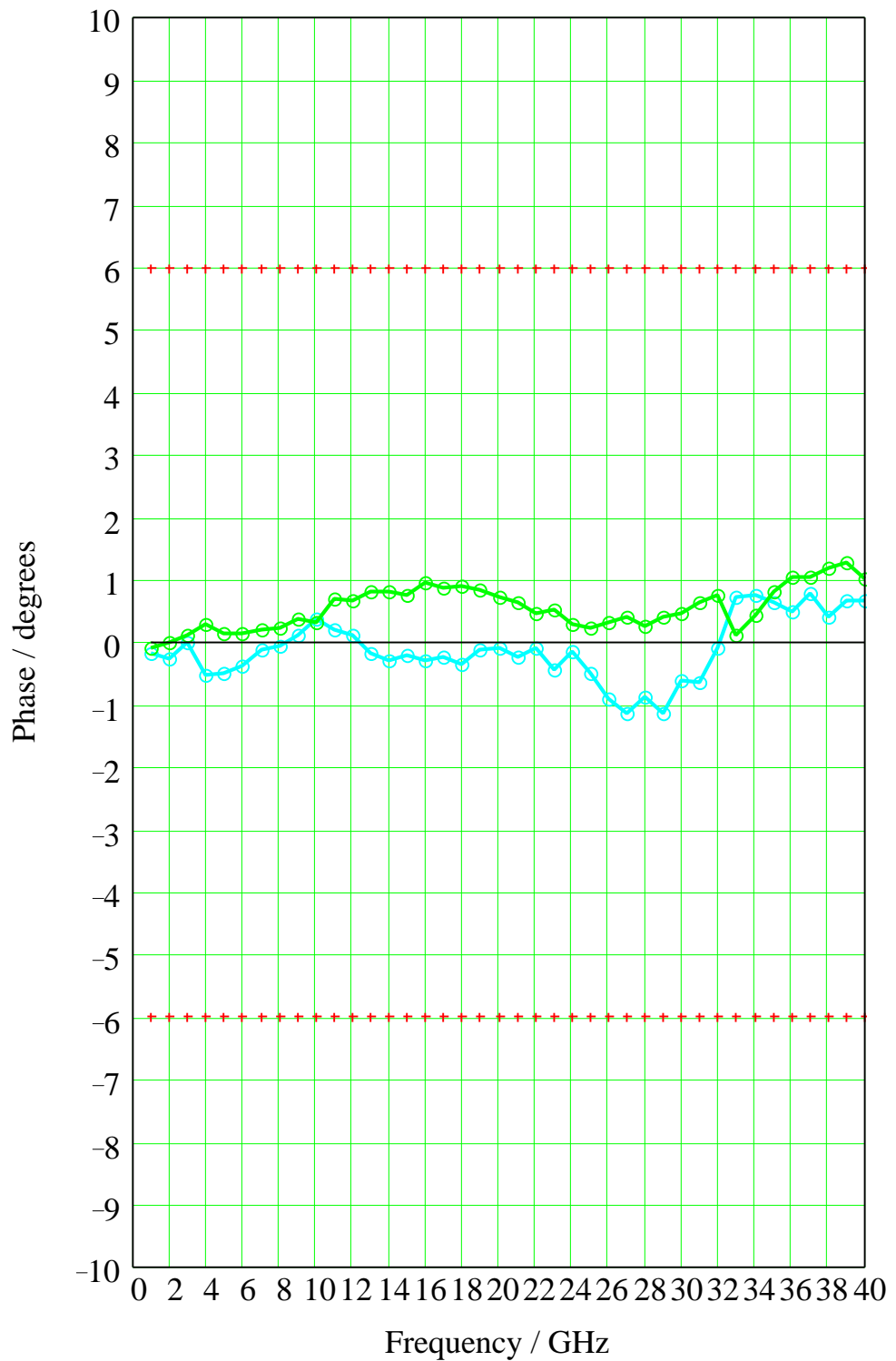
Fig. 5-2   Reflection **phase** deviations: 2.92 mm SHORT verification standard (0 dB)

Verification measurement results of the SHORT standards (blue trace S_{11} of male SHORT, green trace S_{22} of female SHORT) in the frequency range from 1 GHz to 40 GHz. The known electrical lengths of the standards were subtracted and a phase offset of 180° was used. Additionally, the accuracy specifications of ZVK (red crosses) are displayed.
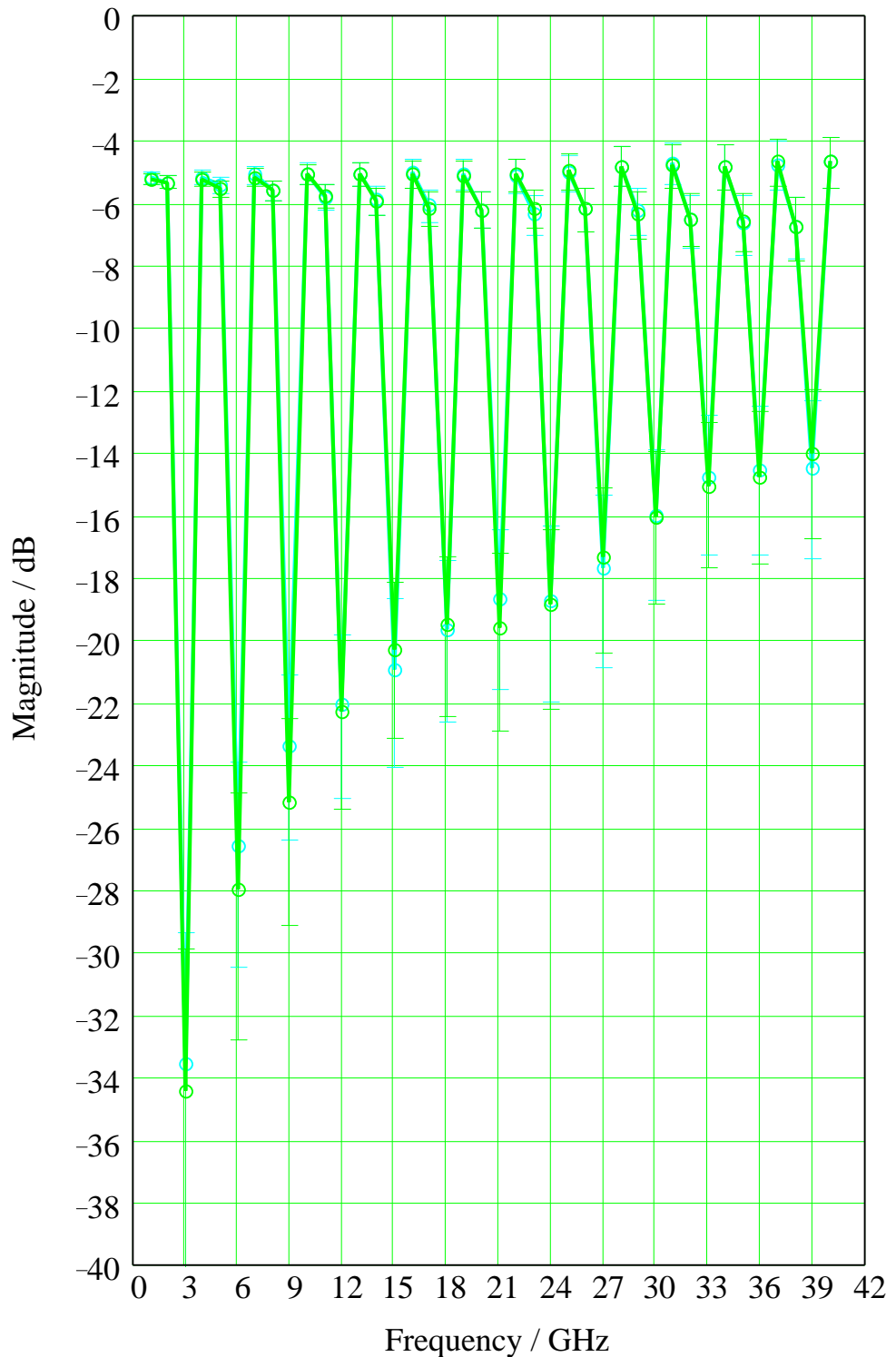
Fig. 5-3   Reflection **magnitude**: 2.92 mm stepped airline verification standard

Magnitude in dB of the reflection coefficients (blue trace S_{11}, green trace S_{22}) of the stepped airline as reported by the manufacturer. Additionally, the reported uncertainties (blue and green bars) are displayed. As can be seen, the matching of the standard is significantly high (in the order of -15 dB to -35 dB) at all multiples of 3 GHz due to the half-wavelength transformation of the 25 Ω section (compare to Fig. 4-18). At the other frequencies, the reflection coefficient is in the order of -5 dB.
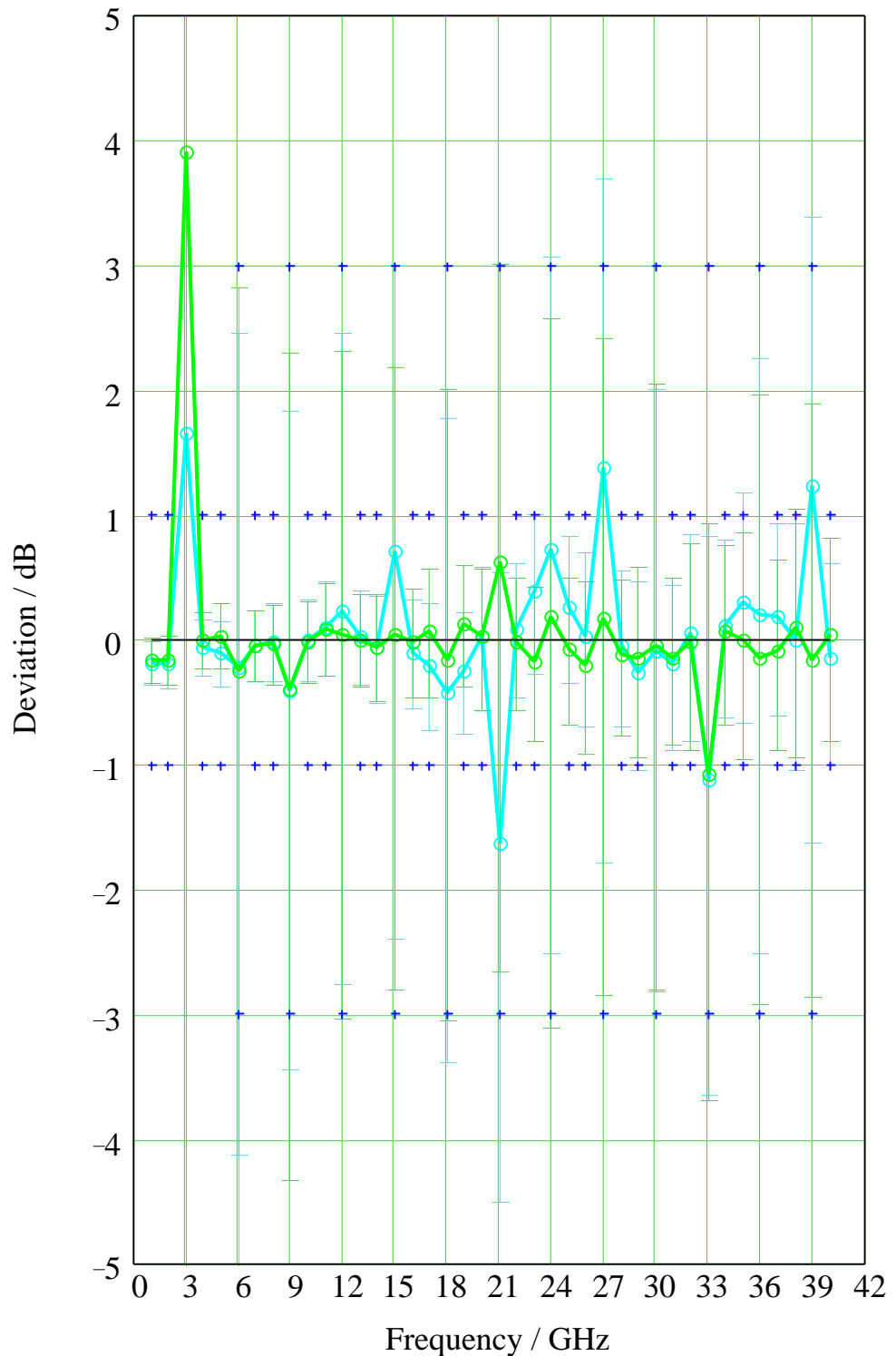
Fig. 5-4   Reflection **magnitude** deviations: 2.92 mm stepped airline verification standard

Differences (blue trace S_{21}, green trace S_{12}) between the verification results obtained by ZVK and the reported data for the stepped airline. Additionally, the reported uncertainties (blue and green bars) are displayed. The accuracy of reflection measurements for non-isolating DUTs is **not specified** in the ZVK data sheet. For information, the ZVK specifications for isolating DUTs with a reflection coefficient - corresponding to the frequency dependent reflection of the Beatty standard - are inserted (blue crosses).
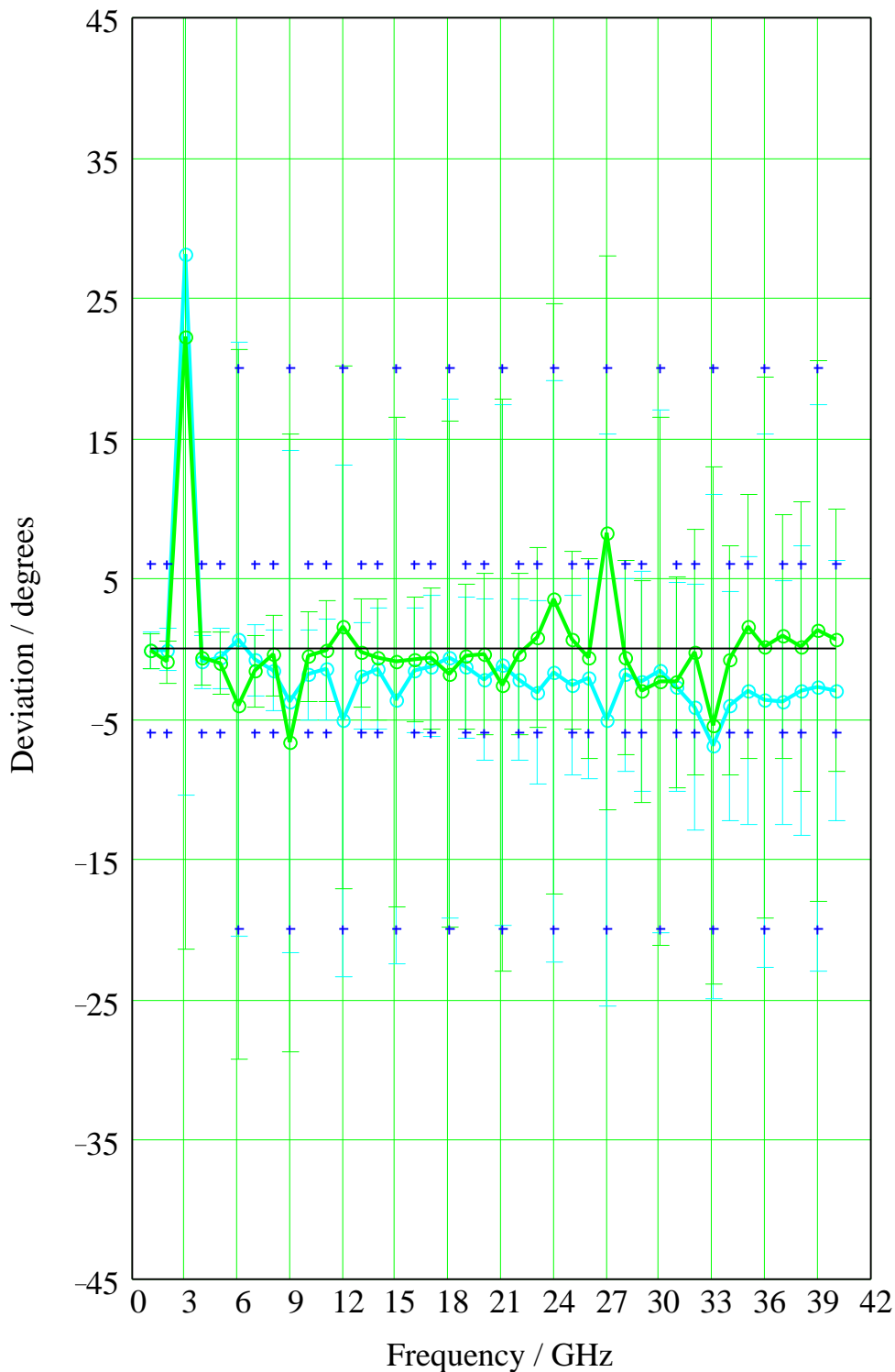
Fig. 5-5   Reflection **phase** deviations: stepped airline verification standard

Differences (blue trace S_{21}, green trace S_{12}) between the verification results obtained by ZVK and the reported data for the stepped airline. Additionally, the reported uncertainties (blue and green bars) are displayed. The accuracy of reflection measurements for non-isolating DUTs is **not specified** in the ZVK data sheet. For information, the ZVK specifications for isolating DUTs with a reflection coefficient corresponding to the frequency-dependent reflection of the Beatty standard are inserted (blue crosses).

6   Effective System Data

The third phase of the verification procedure for the ZVK, was to determine its effective system data. The effective system data describes the residual measurement characteristics of the network analyzer after calibration and system error correction, and can be used to estimate measurement uncertainties for arbitrary but linear devices under test. The effective system data of the ZVK is stated in the data sheet PD 757.5543.22. Twelve different effective system data characterize a two-port network analyzer. Six of them describe the residual characteristics of the analyzer at PORT 1 in forward direction. The other six analogous terms describe the corresponding characteristics at PORT 2 in the reverse direction. The specifications for the corresponding effective system data in forward and reverse direction are identical. For each direction, the following system data are distinguished:

- directivity
- source match
- reflection tracking
- load match
- transmission tracking
- crosstalk.

While the first three are responsible for the accuracy of reflection measurements, the latter three effective system data additionally determine the accuracy of transmission measurements.

For all types of measurements, it should always be considered that a fully error-corrected display of any single S-parameter of a two-port device will be only possible if all its four S-parameters are completely measured.

For the determination of the effective system data, further verification measurements were performed. After TOM-calibration (using sliding MATCHES), reflection measurements at both reference planes were carried out. For that, different one-port standards (OPEN, SHORT, and MATCH) were connected to the reference planes. The 50 Ω airline terminated with a MATCH and, in the other case, terminated with a SHORT was additionally measured for one-port verifications. Furthermore, the two-port verification measurements of the 50 Ω airline standard were repeated, and time-domain transformation was used in addition.

Fig. 6-1 to Fig. 6-9 show the results in the frequency domain and in the time domain.

The measured effective directivity is presented in the Figs. 6-10 and 6-11. The residual source match and the reflection tracking have been calculated from the verification measurements with a SHORT and an OPEN and are illustrated in the Figs. 6-12 to 6-15.

The effective load match was measured with the 50 Ω airline in the time domain using a time gate to suppress the influence of the finite directivity. The time gated results have been re-transformed to the frequency domain and are displayed in Figs. 6-16 and 6-17. Finally, Figs. 6-18 and 6-19 show the evaluation results of the transmission tracking.
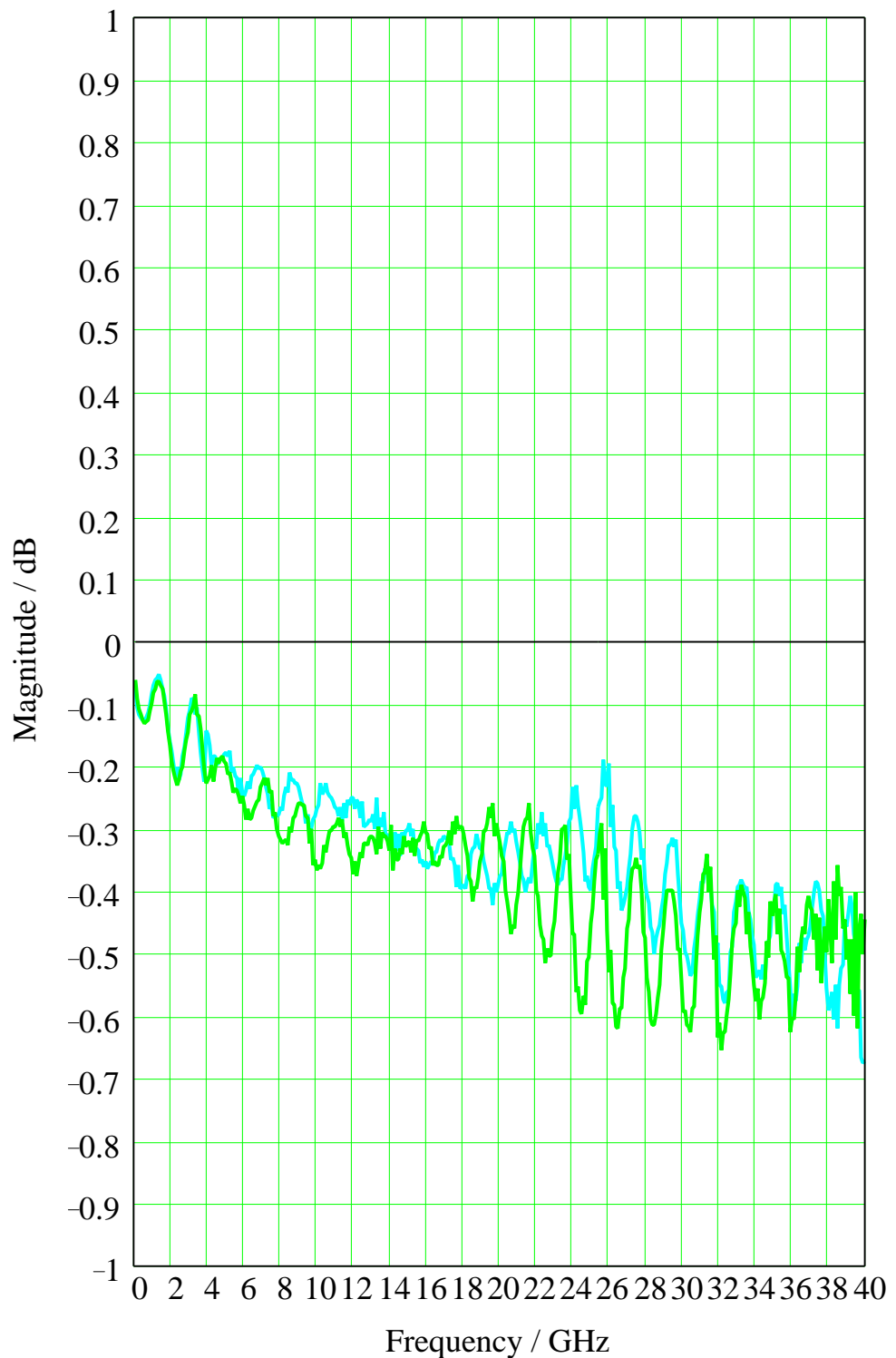
Fig. 6-1   Reflection of the **short circuited 2.92 mm airline** at PORT 1 (blue) and PORT 2 (green)

Reflection response of the 2.92 mm 50 Ω airline short-circuited by the SHORT standard. The observed ripple of maximum ±0.15 dB provides a raw estimation of the effective source match of at least 35 dB. The traces are additionally affected by the finite effective directivity caused by the residual reflection of the MATCH standards. This can be clearly seen in the diagram below 4 GHz where a fixed MATCH with approx. 42 dB return loss was used which leads to a higher ripple than the sliding MATCH above 4 GHz.
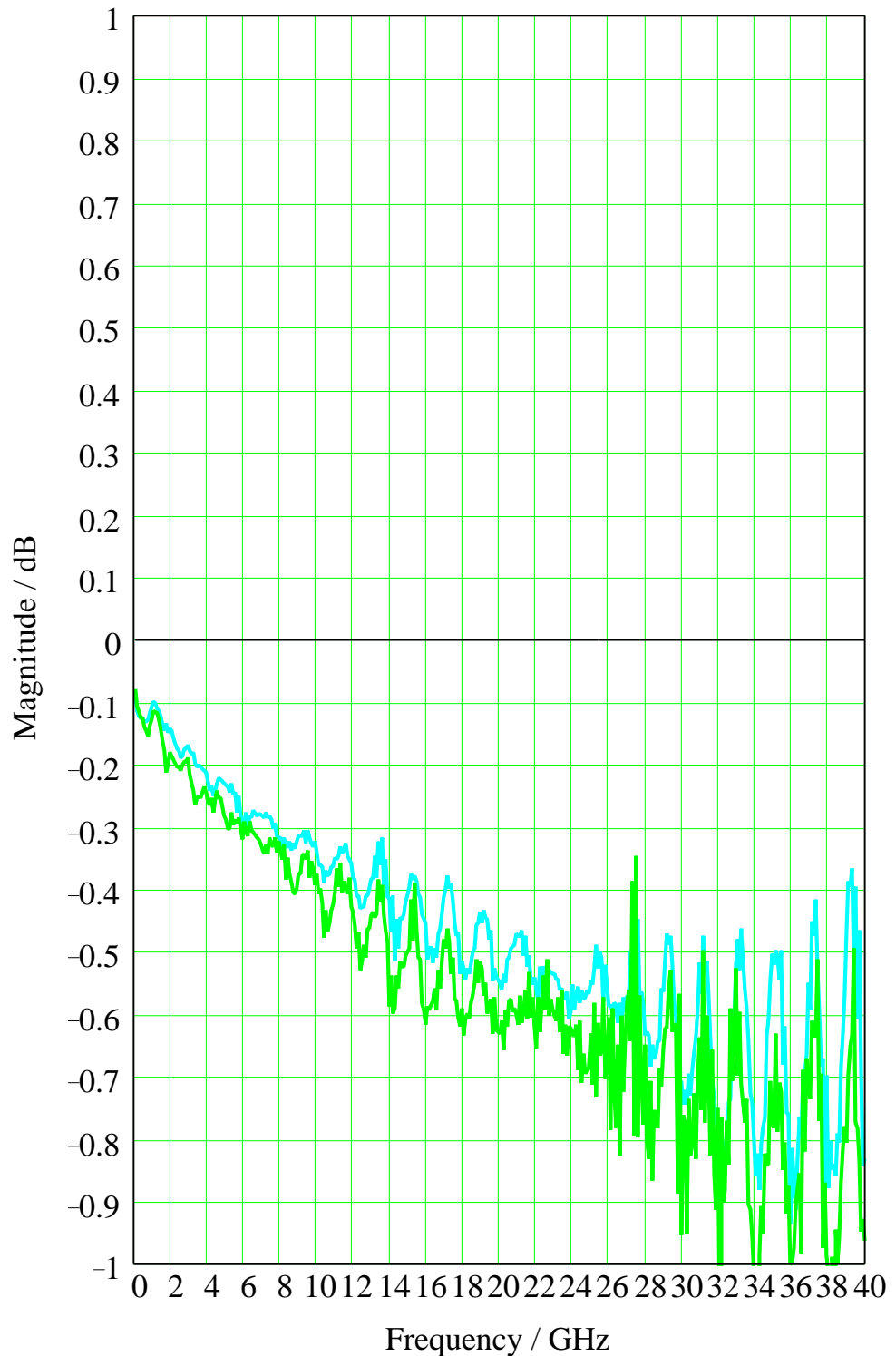
Fig. 6-2   Reflection of the **short circuited 3.5 mm airline** at PORT 1 (blue) and PORT 2 (green)

Reflection response of the 3.5 mm 50 Ω airline short-circuited by the SHORT standard. As the maximum useful frequency for 3.5 mm connectors is 26.5 GHz, the measurement results for frequencies above 26.5 GHz are presented here for information only. Due to the higher quality of the calibration standards of the 3.5 mm calibration kit compared to the 2.92 mm kit, the trace ripple is even less than for the 2.92 mm verification (compare to Fig. 6-1).

```
CH1 S11        LIN MAG 20 U       ↑10 mU
```

Markers:
- ▼1:   -48.96 dB
             -10 ps
- ▽2:   -0.621 dB
     528.822055 ps
- ▽3:   -48.88 dB
     1.005012531 ns

```
START  -1 ns              500 ps/            STOP 4 ns

Date:      23.OCT.00  11:47:47
```

Fig. 6-3   Time domain reflection of the **short circuited 2.92 mm** 50 Ω **airline** at PORT 1

The reflection measurement results of the 2.92 mm 50 Ω airline at PORT 1 after time domain transformation (impulse response). The airline was terminated by the SHORT standard. The frequency range was 100 MHz to 40 GHz.

Three main reflections have occurred. The first impulse (approximately -48 dB) is partly due to the residual **directivity**, and partly to the residual reflection of the not perfectly matched 50 Ω airline. The second impulse (approximately -0.6 dB) represents the unity reflection of the SHORT circuit at the end of the airline reduced by the doubled losses of the airline. The third impulse (approximately -48 dB) is partly due to the residual **source match**, but again, it has also been affected by the finite quality of the 50 Ω airline ($|S_{22}|$ = .008 or -42 dB at 40 GHz, see Table 1-1). Due to the length of the airline (75 mm), the individual impulses show a time delay of 500 ps.

CH1 S11 LIN MAG 20 U ↑10 mU

▼1:	−65.24 dB
	12.5 ps
▽2:	−0.539 dB
	562.5 ps
▽3:	−56.76 dB
	1.05 ns

10 mU

TIM

CAI

1 mU/

CPL

3

FIL
100

0 U

START −1 ns 500 ps/ STOP 4 ns

Date: 2.NOV.00 16:41:22

Fig. 6-4 Time domain reflection of the **short circuited 3.5 mm** 50 Ω **precision airline** at PORT 1

The reflection measurement results of the **3.5 mm** 50 Ω precision airline at PORT 1 after time domain transformation (impulse response). The airline was terminated by the SHORT standard. The frequency range was 100 MHz to 20 GHz.

Three main reflections can be observed. The first impulse (approximately -65 dB) is due to the residual **directivity**, the second one (approx. -0.5 dB) to the unity reflection of the SHORT circuit at the end of the airline reduced by the doubled losses of the airline. The third impulse (approximately -56 dB) results from the residual **source match**. The length of the airline (75 mm) leads to a time delay of 500 ps between the individual impulses.

The reflected impulses are significantly lower than those in the 2.92 mm airline (see Fig. 6-3) due to;

- lower frequency range (100 MHz to 20 GHz instead of 100 MHz to 40 GHz)

- higher quality of the 3.5 mm precision airline (approx. -58 dB at 20 GHz, as stated in Table 3-3, p. 4 instead of -42 dB at 40 GHz of the 2.92 mm airline, as stated in Table 3-1, p. 3)

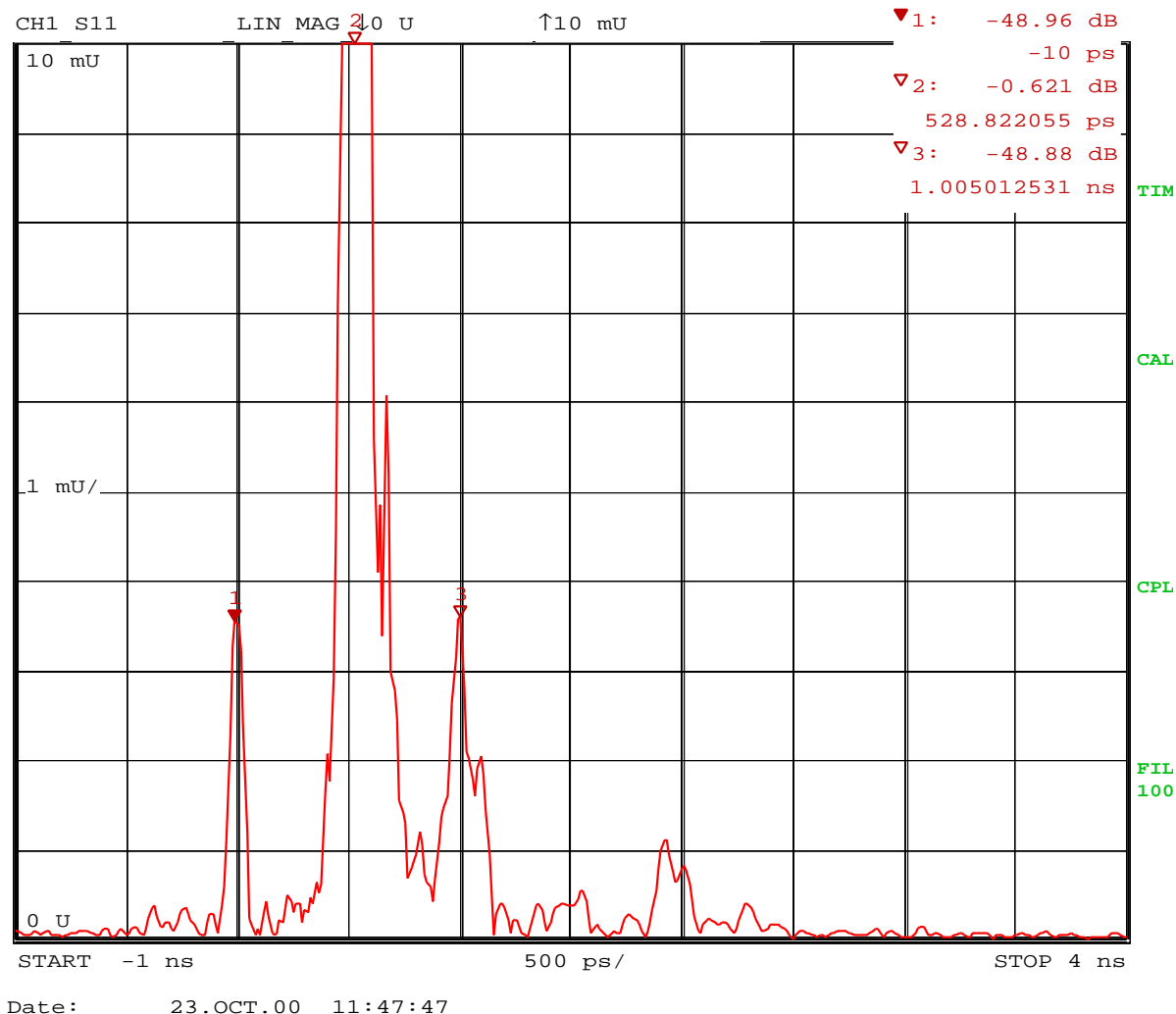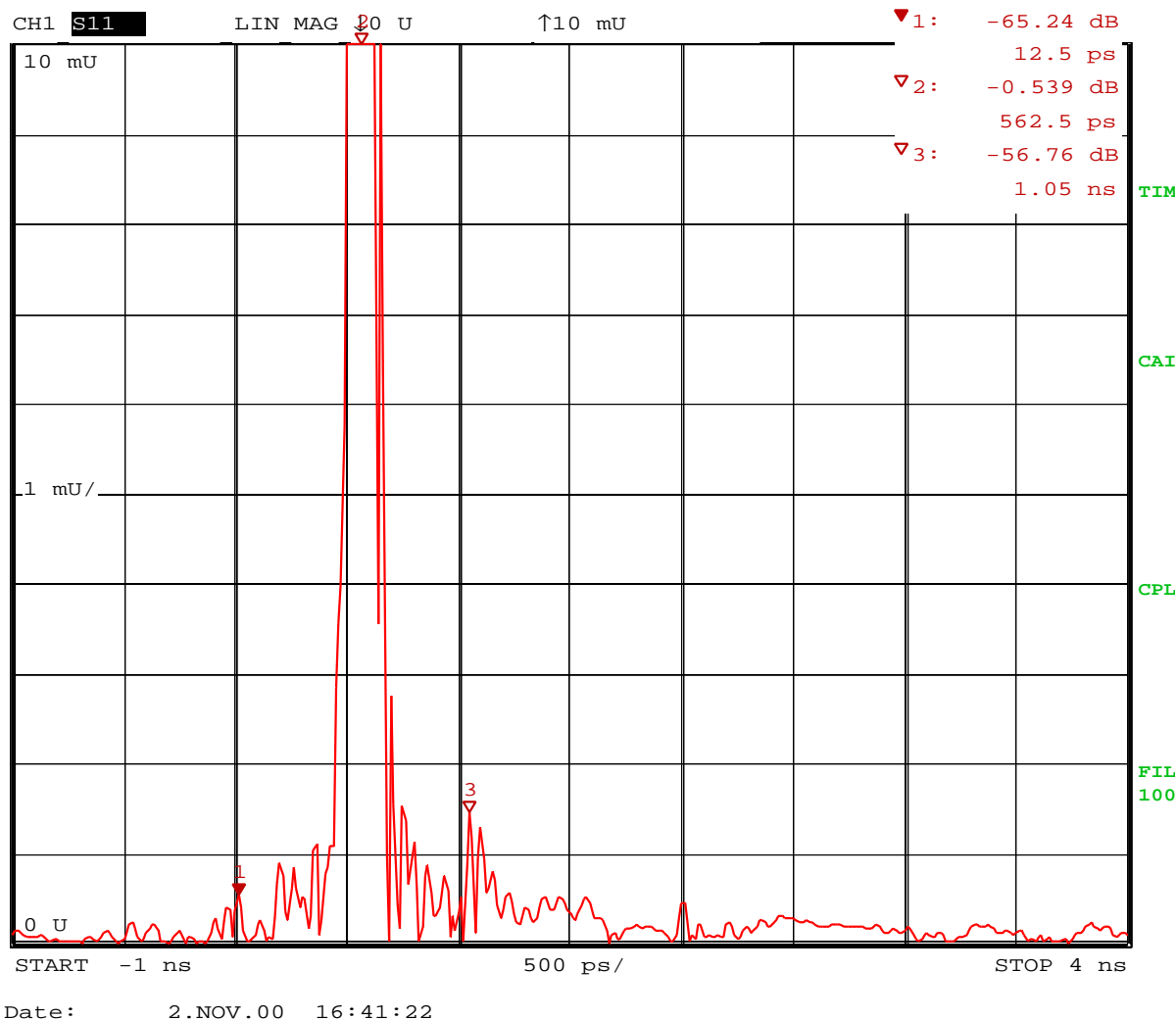- higher quality of the 3.5 mm calibration standards in comparison to the 2.92 mm standards.

Fig. 6-5   Time domain reflection of the **terminated 2.92 mm airline** at PORT 1

The reflection measurement results of the 2.92 mm 50 Ω airline at PORT 1 after time domain transformation (impulse response). The airline was terminated by the **2.92 mm fixed MATCH** standard. The frequency range was 100 MHz to 40 GHz.

Three main reflections have occurred. The first impulse (approximately -48 dB) is due to the impedance step at the near end of the airline and to the residual **directivity**. The second one (approximately -47 dB) is due to the discontinuity at the end of the airline connected to the MATCH standard. The third impulse has been a result of the MATCH standard itself. As can clearly be seen, the reflection coefficient of the MATCH standard (approximately -30 dB) is far from being ideal. For this reason, sliding MATCHES or precision AIRLINES (TRL method) are generally preferred as calibration standards to achieve a high directivity.

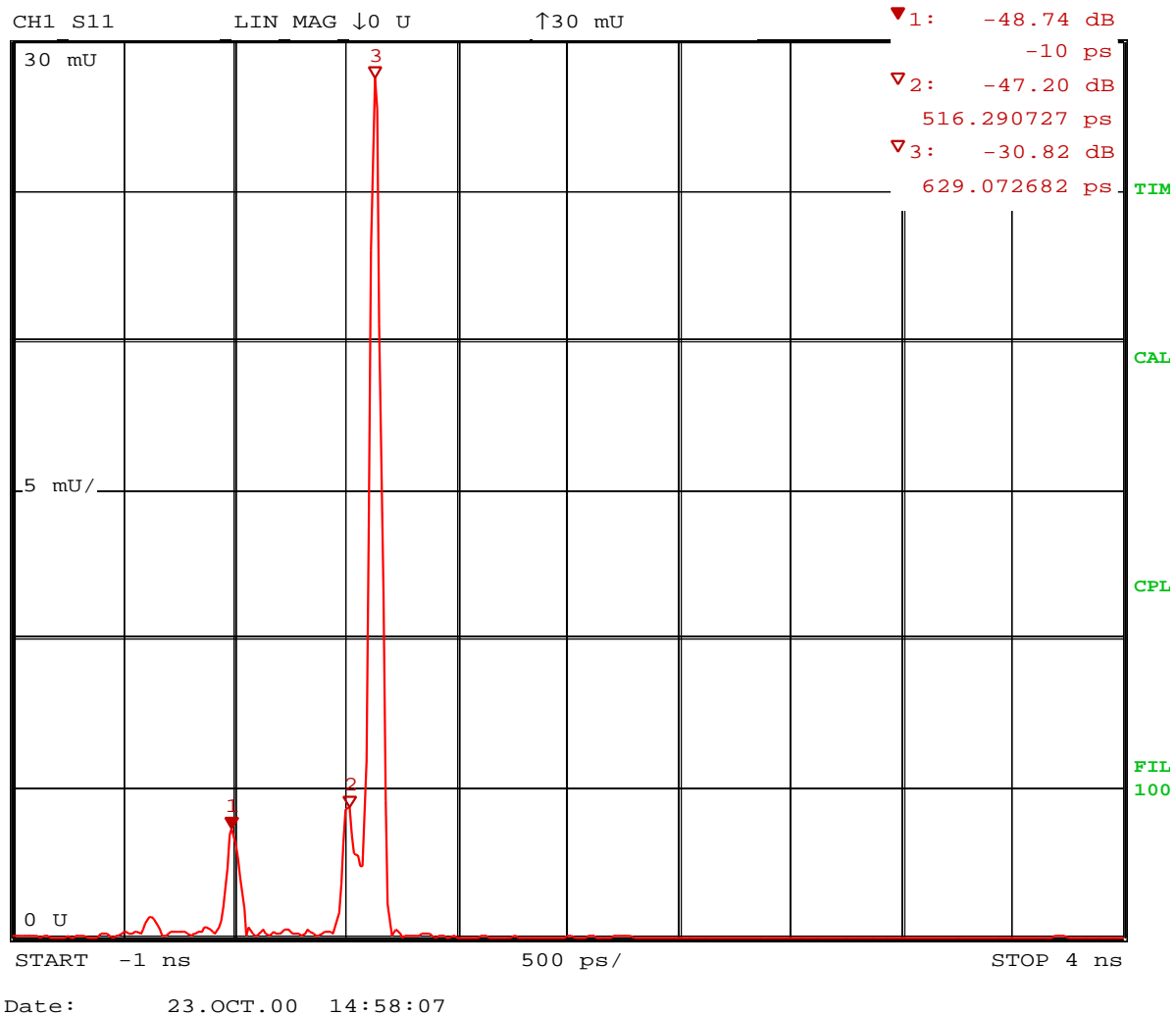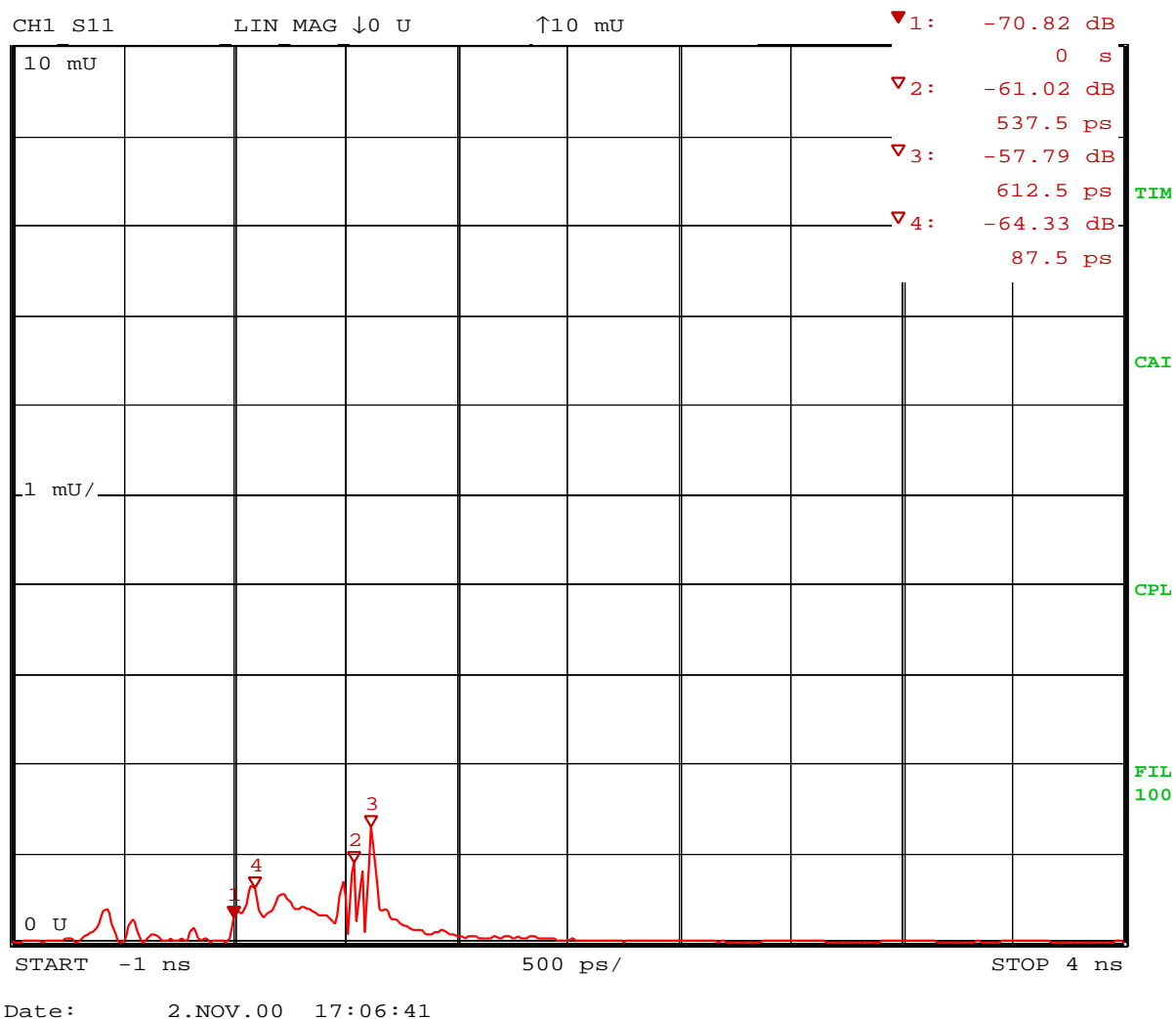Fig. 6-6   Measured time domain reflection of the **terminated 3.5 mm precision airline** at PORT 1

The reflection measurement results of the 3.5 mm 50 Ω precision airline at PORT 1 after time domain transformation (impulse response). The airline was terminated by the 3.5 mm fixed MATCH standard of the 3.5 mm calibration kit. The frequency range was 100 MHz to 20 GHz.

It is remarkable that the residual reflections are of a far smaller degree than those illustrated in Fig. 6-5. This is partly due to the lower frequency range (100 MHz to 20 GHz instead of 100 MHz to 40 GHz). But the main reason is the higher quality of the 3.5 mm calibration standards and, especially, the precision of the 3.5 mm airline compared to the 2.92 mm components.

Four reflections have been observed. The first impulse (approximately -70 dB) is again due to the residual **directivity**. Impulse number ∇2 (approx. -61 dB) is caused by the discontinuity at the end of the airline connected to the MATCH standard, while impulse ∇3 (approximately -58 dB) is due to the MATCH standard itself. Its reflection coefficient is much smaller than that of the 2.92 mm standard as presented in Fig. 6-5.

Unlike the 2.92 mm airline used for the measurement results presented in Fig. 6-5, the 3.5 mm airline - applied to this verification measurement - contains a dielectric support adjacent to the near end of the airline. Although this dielectric support is very well compensated and its reflection is nearly negligible, the ZVK is, however, capable of detecting it, as clearly illustrated in the diagram at marker ∇4 (approximately -64 dB).

```
CH1  S11          LIN MAG ↓0 U          ↑10 mU                ▼1:    -68.17 dB
                                                                     12.5 ps
 10 mU                                                        ▽2:    -58.33 dB
                                                                     532.5 ps
                                                             ▽3:     -58.75 dB
                                                                     610 ps    TIM
                                                             ▽4:     -66.85 dB
                                                                     90 ps
                                                                               CAI
 1 mU/
                                                                               CPL
                                                                               FIL
                                                                               100
 0 U
 START  -1 ns                       500 ps/                  STOP 4 ns
 Date:       6.NOV.00   15:42:49
```
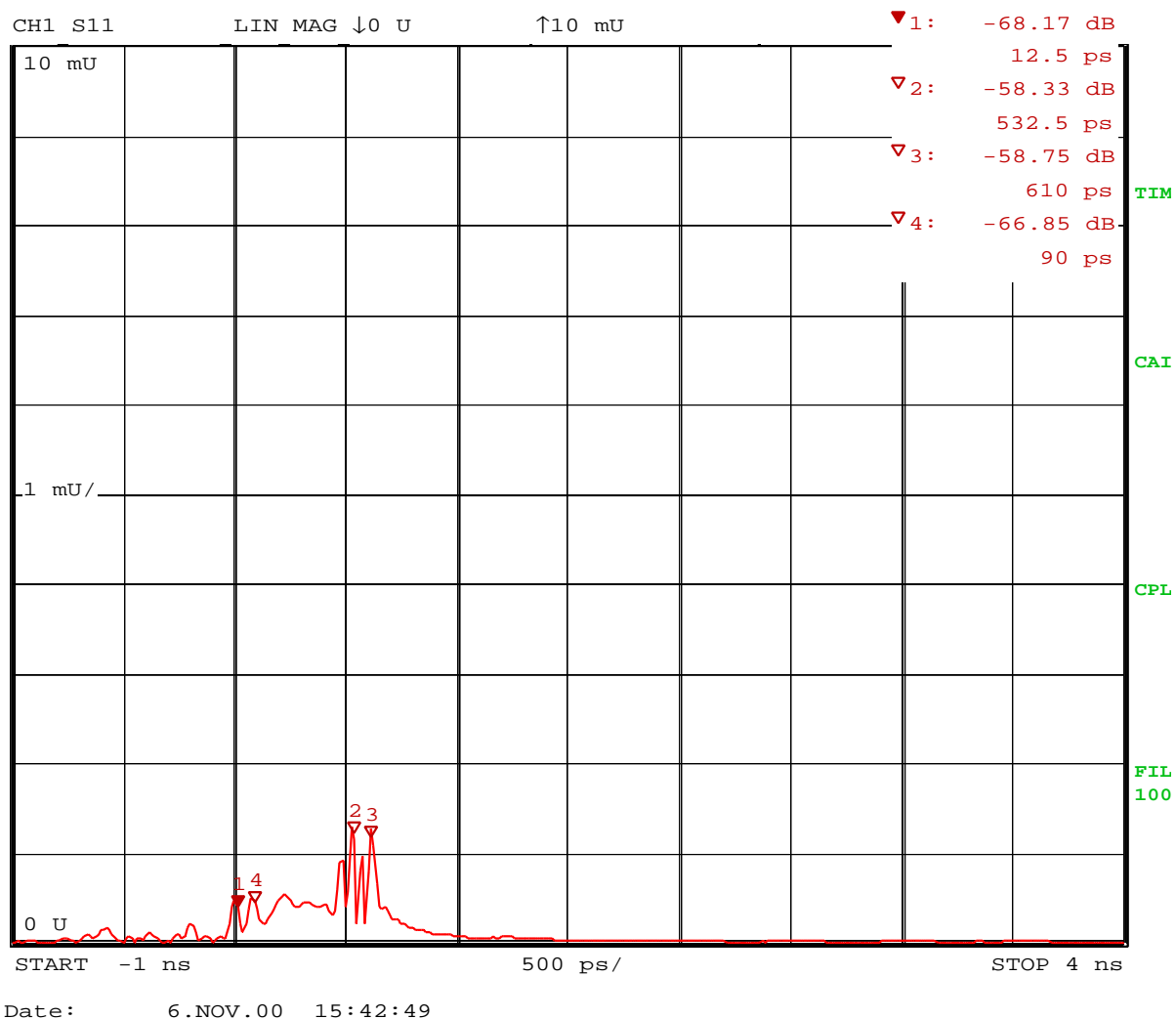
Fig. 6-7   Measured time domain reflection of the **terminated 3.5 mm precision airline** at PORT 1

As already illustrated in Fig. 6-6, this presentation again shows the reflection measurement results of the 3.5 mm precision airline at PORT 1 after time domain transformation (impulse response). The measurement setup is the same as for Fig. 6-6, with the exception that the measurement was performed **four days later**. The airline standard had been disconnected for four days and was then re-connected. No new calibration was performed.

The high similarity of the measurement results compared to Fig. 6-6 is a good indication of the high stability of the ZVK and the excellent repeatability of the connections.

All the measurements presented in this application note were performed in a laboratory without air-conditioning system and under natural ambient conditions.

```
CH1 S11        LIN MAG ↓0 U        ↑20 mU              ▼1:    -47.29 dB
                                                           -11.111111 ps
                                                       ▽2:    -51.71 dB
                                                           516.666667 ps
                                                       ▽3:    -36.20 dB
                                                           916.666667 ps   TIM
```



```
START  -500 ps               200 ps/                    STOP 1.5 ns
Date:      23.OCT.00  15:23:26
```
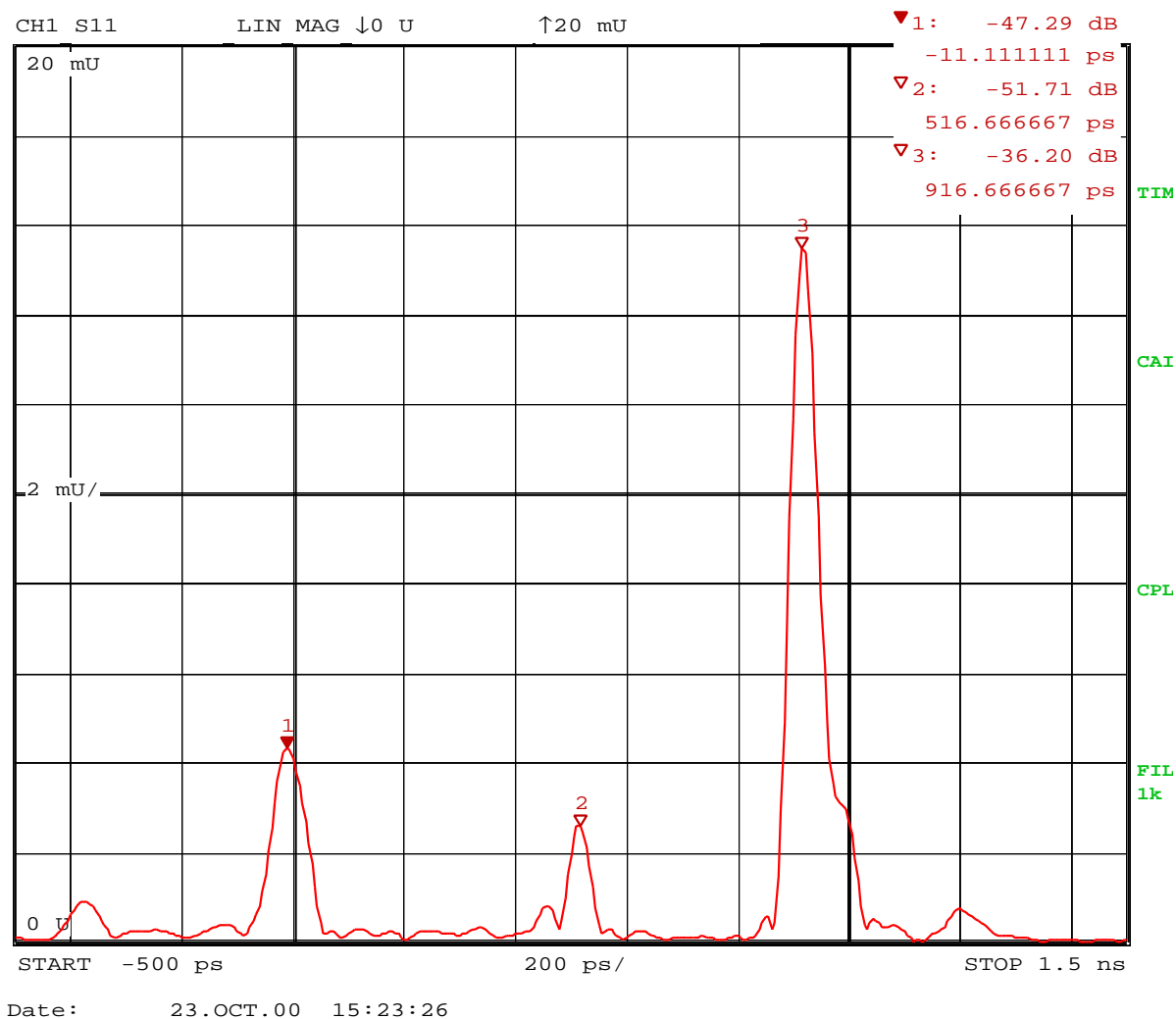
Fig. 6-8   Time domain reflection of the **terminated 2.92 mm** 50 Ω **airline** at PORT 1

The reflection measurement results of the 50 Ω airline at PORT 1 after time domain transformation (impulse response). The airline was terminated by the **2.92 mm sliding MATCH** standard. The frequency span was narrowed down to the range from 4 GHz to 40 GHz to take the finite operating range of the sliding MATCH into account.

Three main reflections have occurred. The first impulse (approximately -47 dB) is again partly generated by the residual reflection of the airline and partly due to the residual **directivity**, the second one (approximately -52 dB) to the discontinuity at the end of the airline connected to the sliding MATCH standard. The third impulse (approximately -36 dB) results from the reflection of the ferrite element within the sliding MATCH.

```
CH1 S22          LIN MAG ↓0 U          ↑10 mU          ▼1:    -49.72 dB
                                                              13.888889 ps
                                                        ▽2:    -48.50 dB
                                                              972.222222 ps
```
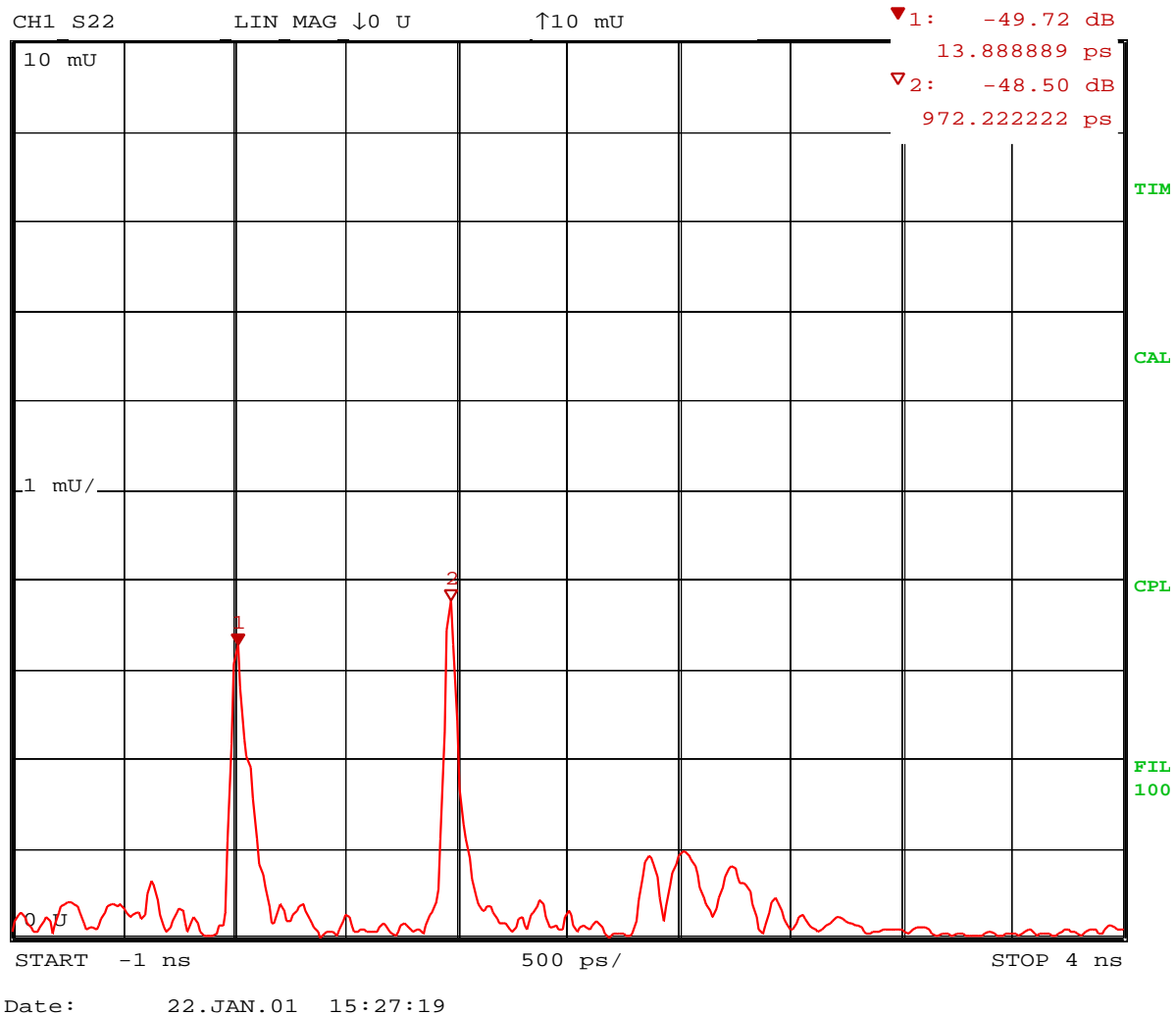
Fig. 6-9   Time domain reflection of a 2.92 mm **airline** calibration standard

The reflection measurement results of a 2.92 mm airline directly connected to both calibrated reference planes of PORT 1 and PORT 2. For this measurement an airline from Maury Microwave Corporation (Model 8774C15) with a length of 149.90 mm was used.

Two main reflections have occurred. The first impulse (approximately -50 dB) is partly due to the residual **directivity**. It is affected by the finite reflection coefficient at the near end of the airline verification standard. The second impulse (approximately -48 dB) is partly caused by the finite **load match** of the network analyzer. The impulse is additionally affected by the finite reflection coefficient at the far end of the airline.
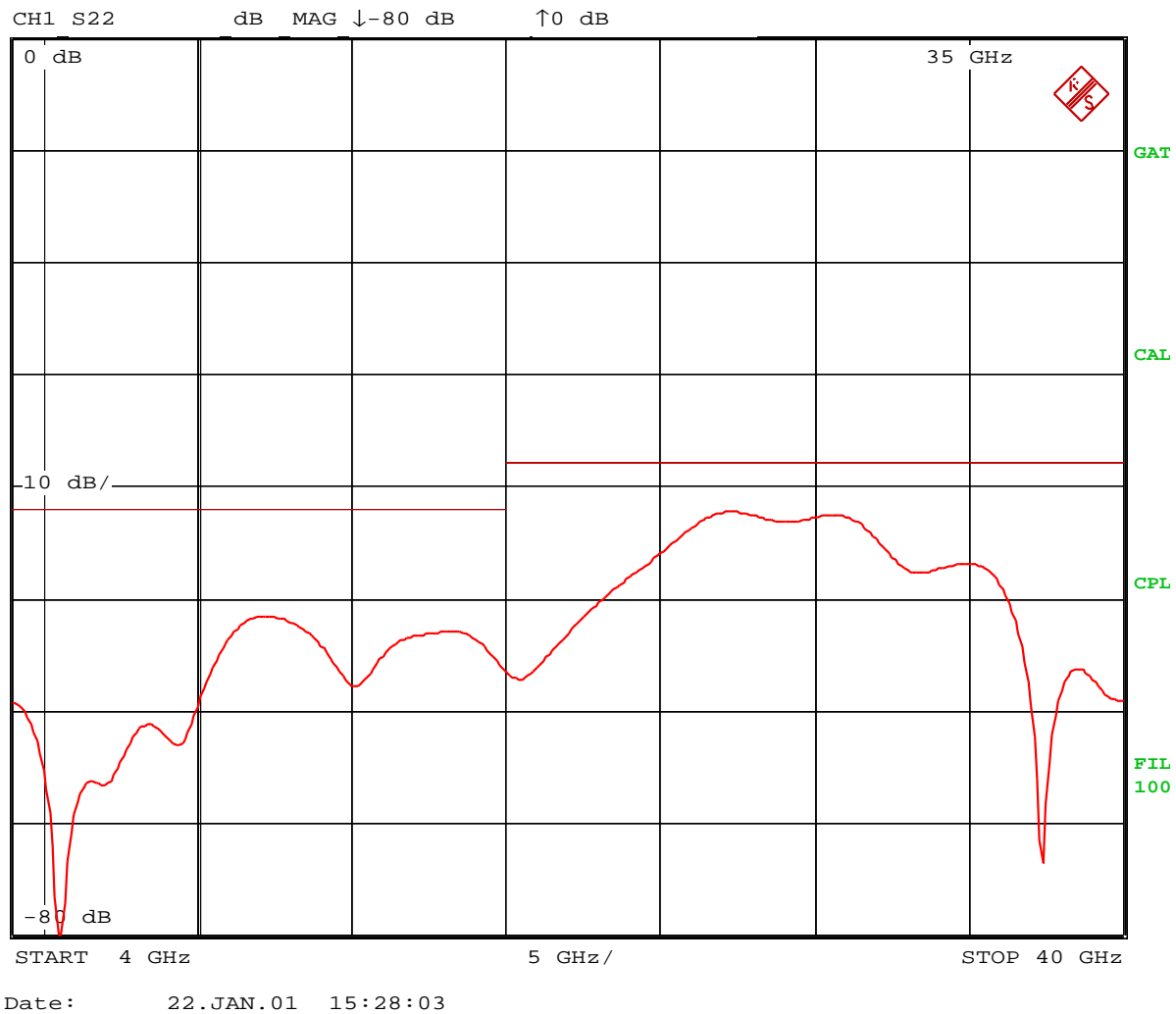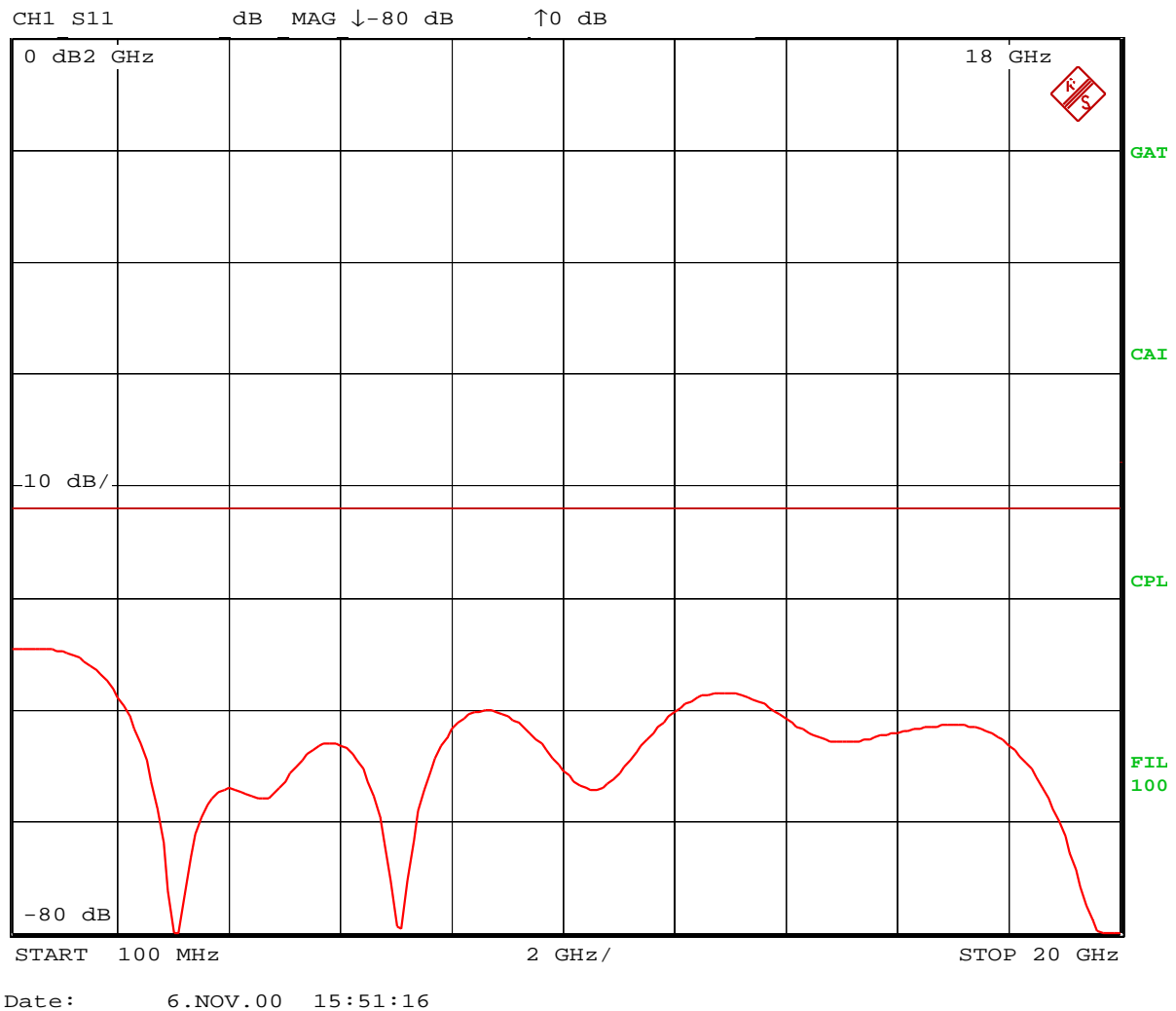
Fig. 6-10   Residual **directivity** in dB vs. frequency in GHz after **2.92 mm** calibration

The time domain measurement results of Fig. 6-9 were gated with a time gate at 0 s and a time span of 500 ps to remove the effects from the far end of the airline and to focus on the residual directivity of the system.

The displayed measurement results are partly affected by the finite matching of the airline.

```
CH1 S11          dB  MAG ↓-80 dB      ↑0 dB
```



```
0 dB2 GHz                                    18 GHz
                                                      GAT

                                                      CAI

10 dB/
                                                      CPL

                                                      FIL
                                                      100

-80 dB
START  100 MHz              2 GHz/            STOP 20 GHz
```

```
Date:      6.NOV.00  15:51:16
```

Fig. 6-11   Residual **directivity** in dB vs. frequency in GHz after **3.5 mm** calibration

The time domain measurement results of Fig. 6-7 were gated with a time gate at 0 s and a time span of 500 ps to remove the effects of the MATCH at the far end of the 50 Ω precision airline and to focus on the directivity of the system.

The displayed measurement results are partly affected by the finite matching of the airline.
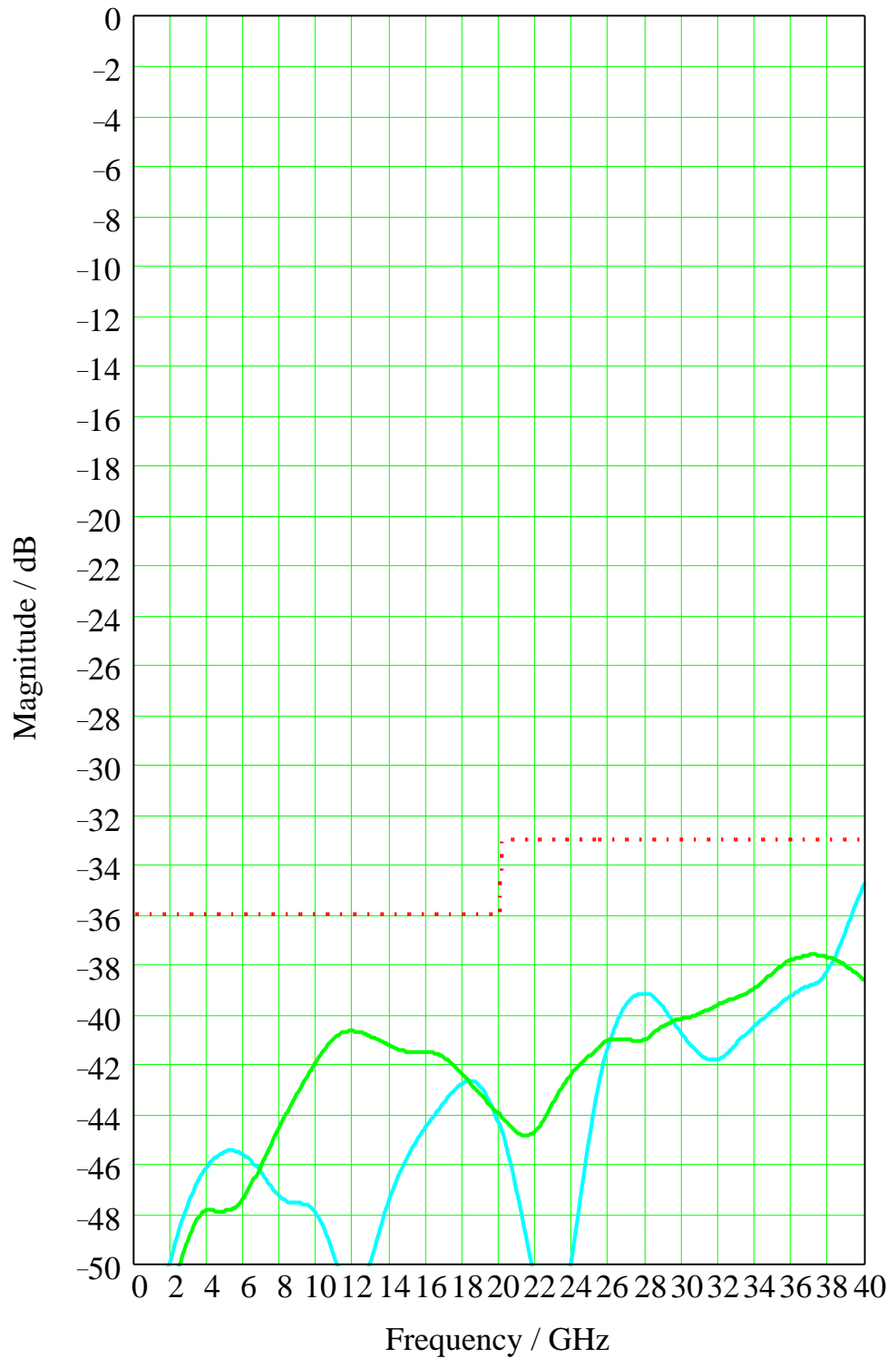
Fig. 6-12   Residual **source match** in dB vs. frequency in GHz after a **2.92 mm** calibration

The effective source match was evaluated via verification measurements with an OPEN, SHORT, and MATCH. The results are partly affected by the residual errors of the capacity model of the OPEN standard and the finite matching of the MATCH standard.
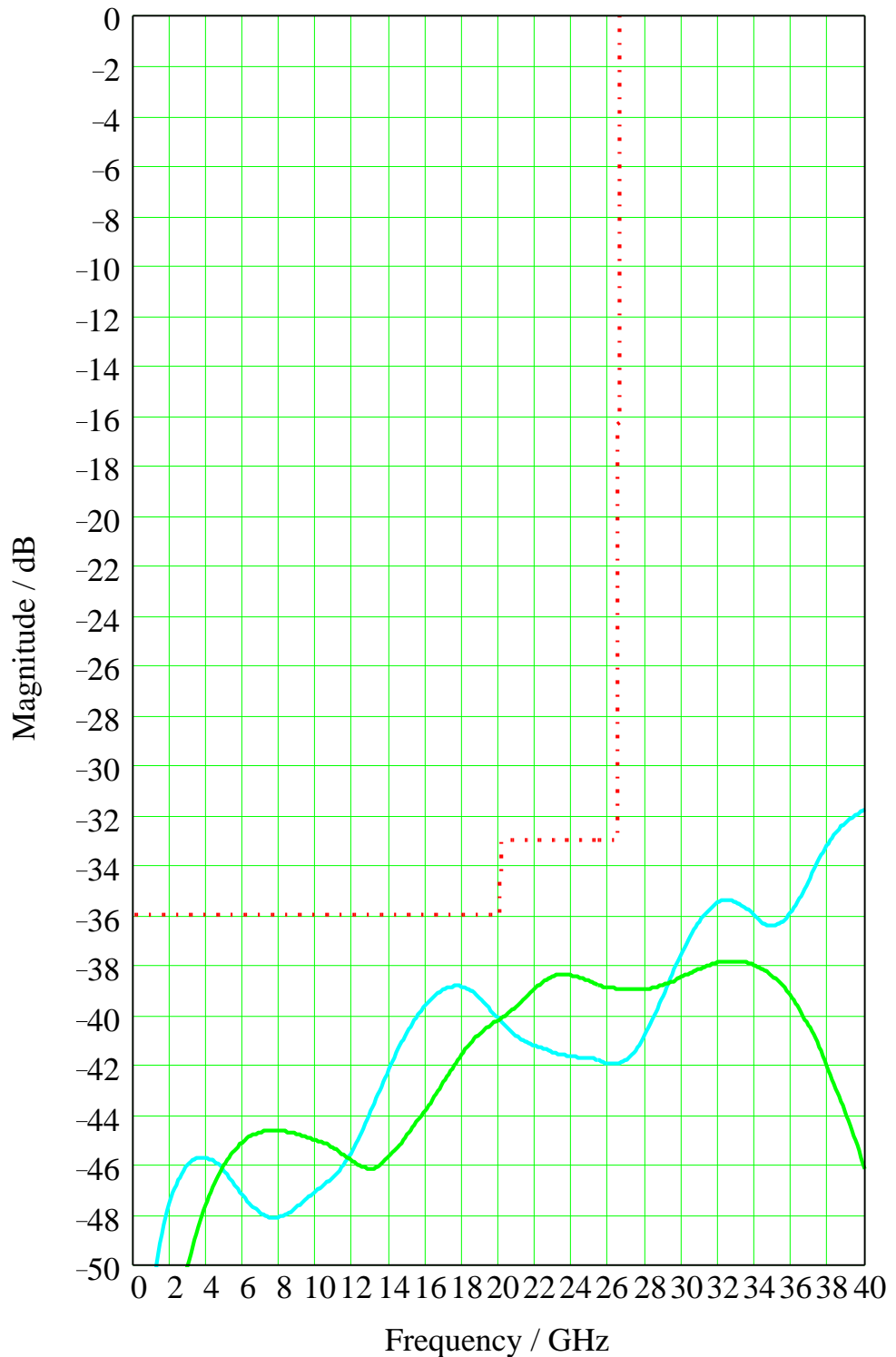
Fig. 6-13   Residual **source match** in dB vs. frequency in GHz after a **3.5 mm** calibration

The effective source match was evaluated via verification measurements with an OPEN, SHORT, and MATCH. As already stated for Fig. 6-12, the results are partly affected by the residual errors of the capacity model of the OPEN standard and the finite matching of the MATCH standard.

Measurement results for frequencies above 26.5 GHz are presented for information only, as the maximum useful frequency for 3.5 mm connectors is 26.5 GHz.
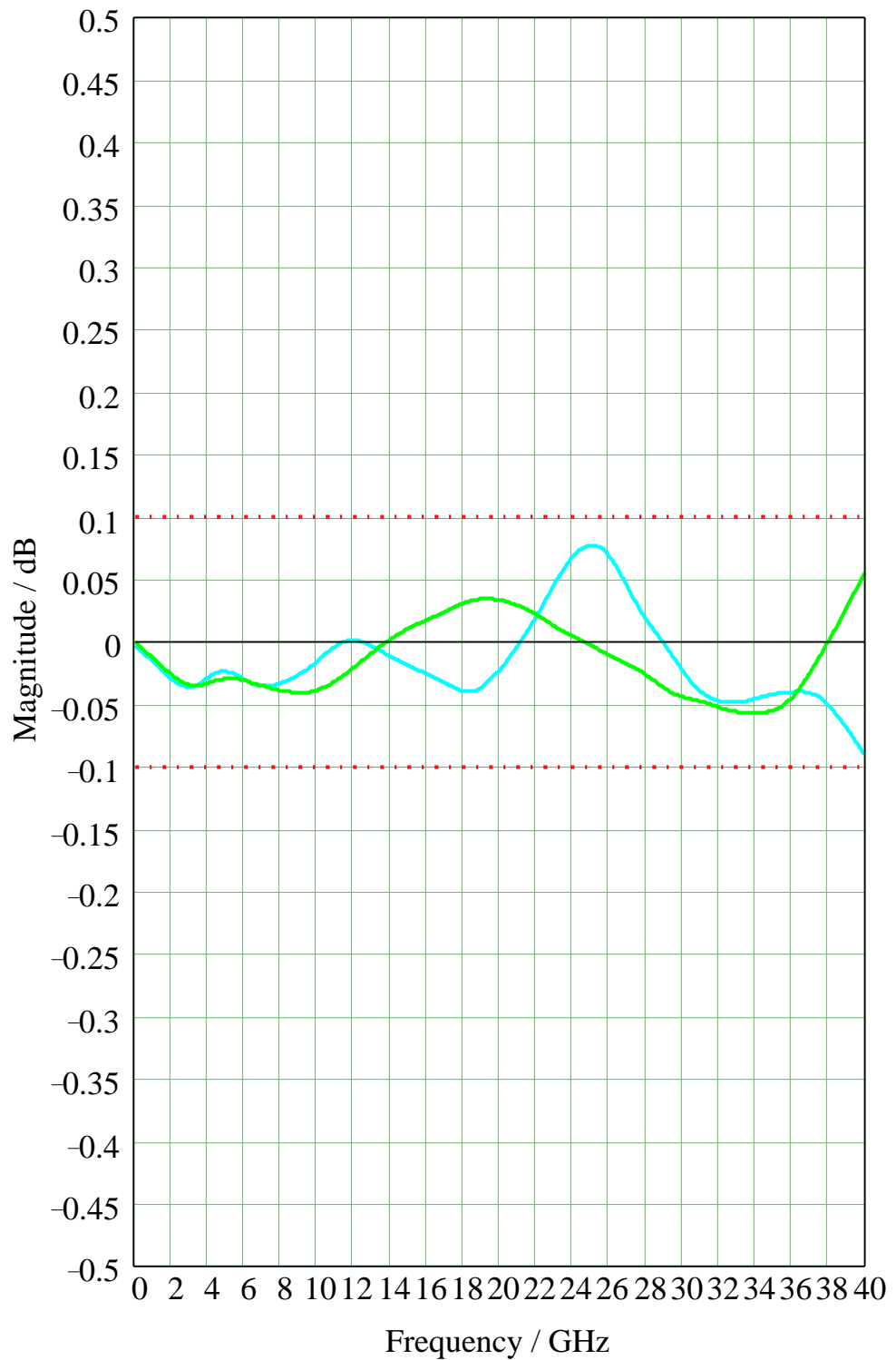
Fig. 6-14   Residual **reflection tracking** in dB vs. frequency in GHz after a **2.92 mm** calibration

The reflection tracking was evaluated via verification measurements with an OPEN, SHORT, and MATCH. The results are partly affected by the residual errors of the capacity model of the OPEN standard and the finite matching of the MATCH standard.
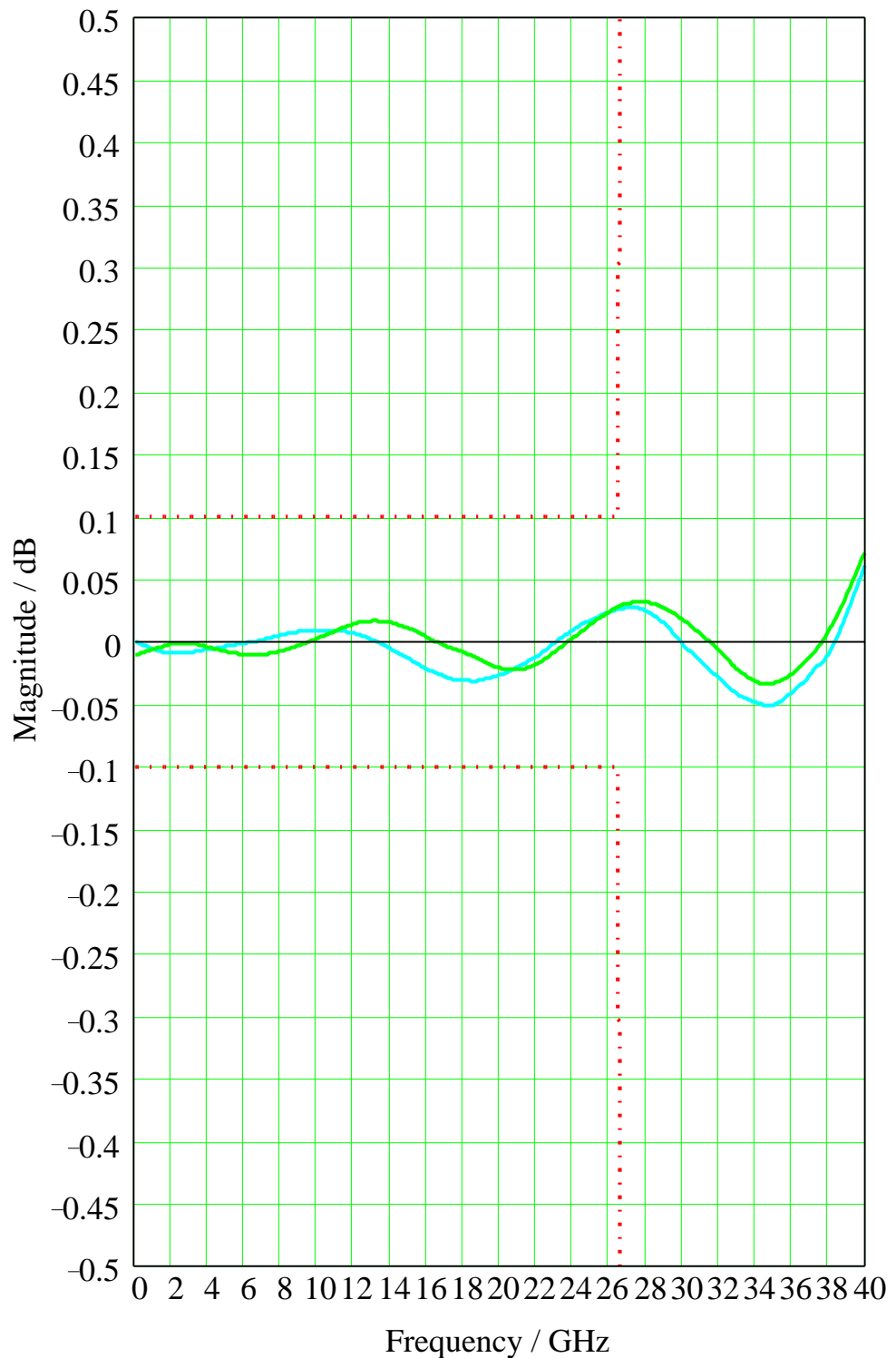
Fig. 6-15   Residual **reflection tracking** in dB vs. frequency in GHz after a **3.5 mm** calibration

The reflection tracking was evaluated via verification measurements with an OPEN, SHORT, and MATCH. As already stated for Fig. 6-14, the results are partly affected by the residual errors of the capacity model of the OPEN and the finite matching of the MATCH standards.

Again, measurement results for frequencies greater than 26.5 GHz are presented for information only.

CH1 S22   dB MAG ↓-80 dB   ↑0 dB

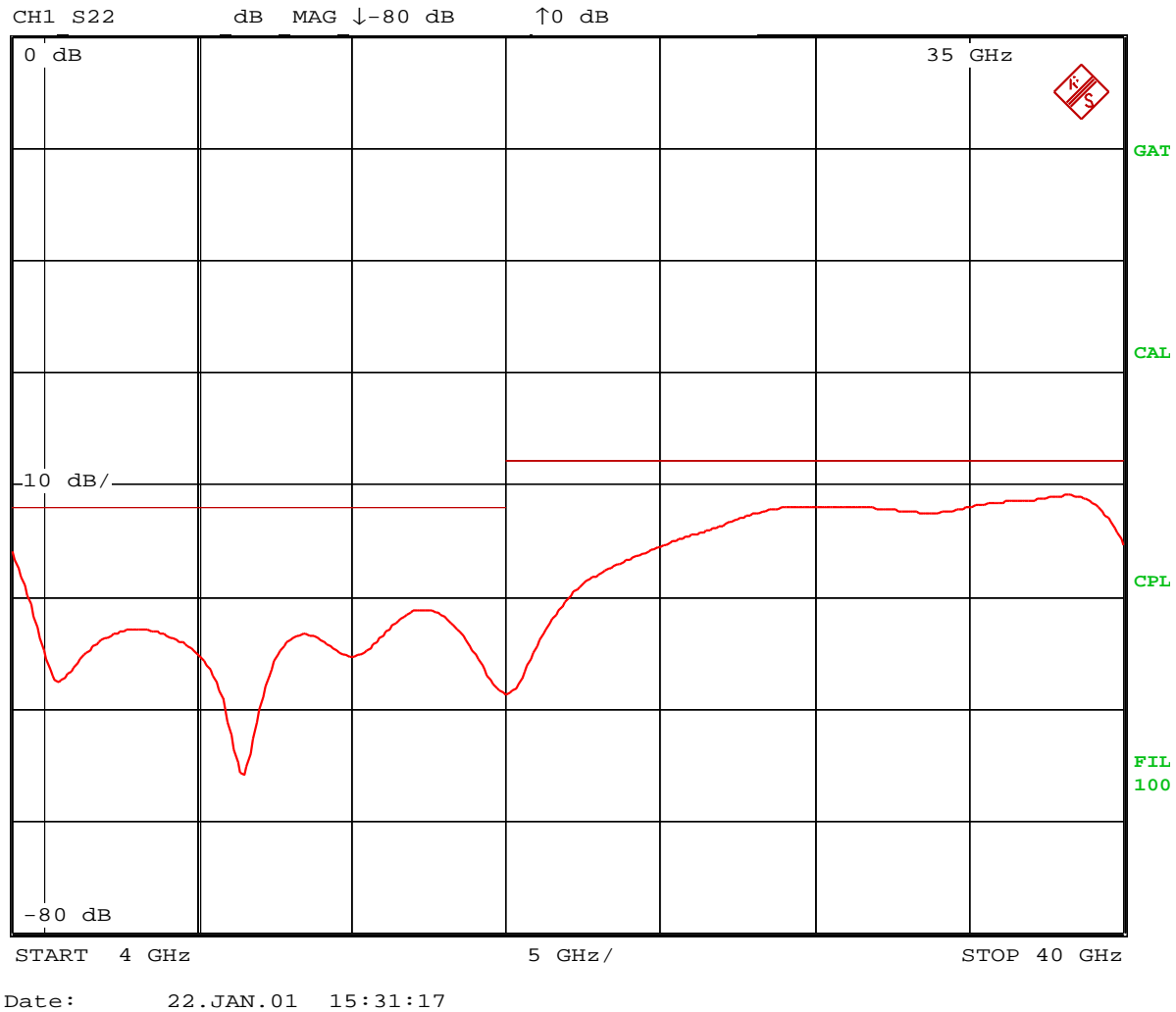Date: 22.JAN.01   15:31:17

Fig. 6-16   Residual **load match** in dB vs. frequency in GHz after **2.92 mm** calibration

The displayed results were obtained via the verification measurement with the 50 Ω airline standard between both measurement PORTs, as shown in Fig. 6-9. The effects of the finite directivity have been removed by a time gate (gate center = 1 ns, gate span = 500 ps).

The displayed measurement results are partly affected by the finite matching of the airline.

CH1 S11   dB MAG ↓-60 dB   ↑0 dB


```
 0 dB   5 GHz                                            35 GHz
```

GAT

CAL

-5 dB/

CPL

FIL
100

-60 dB

```
START  100 MHz                    5 GHz/                    STOP 40 GHz
```
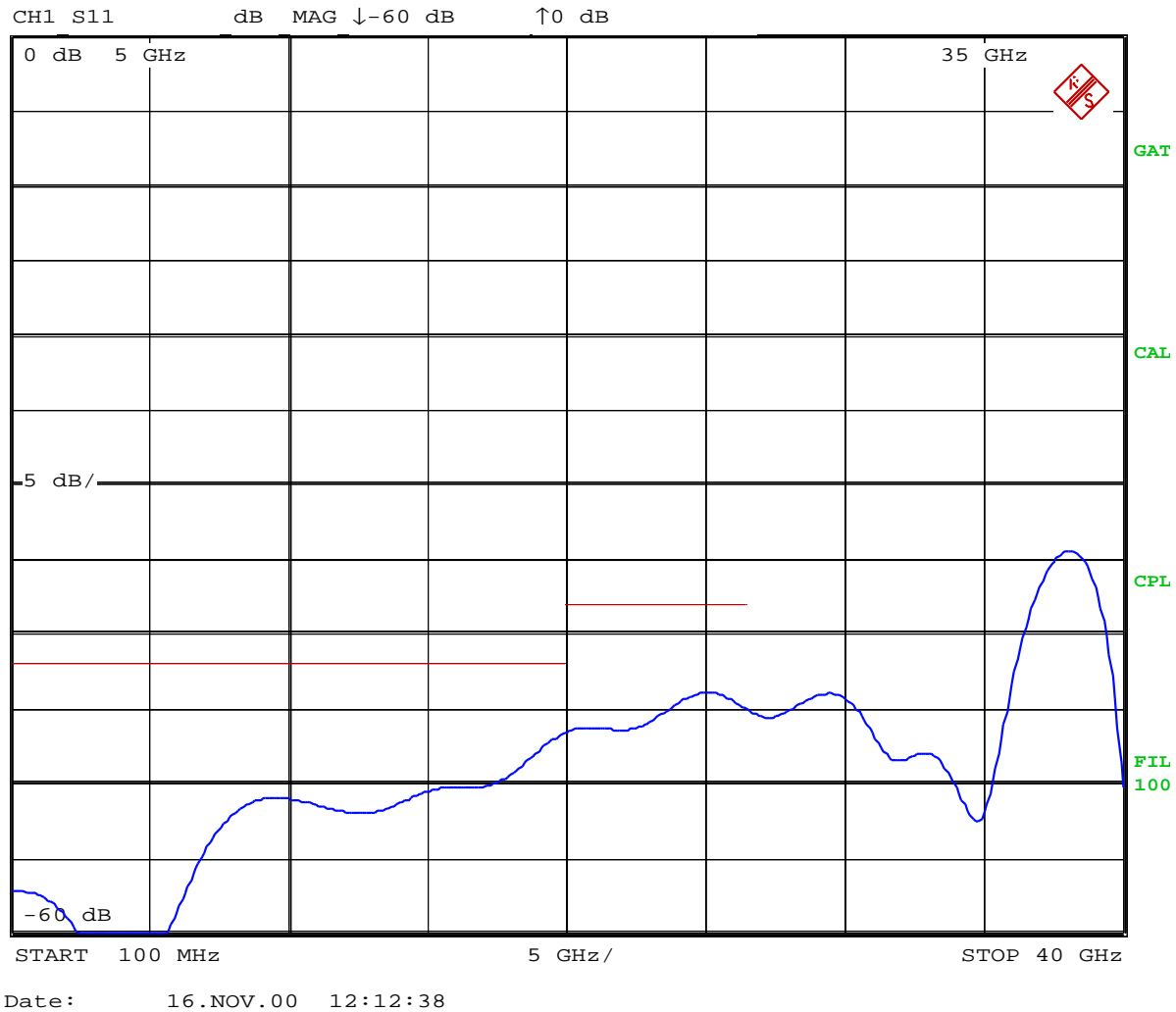
Date: 16.NOV.00 12:12:38

Fig. 6-17   Residual **load match** in dB vs. frequency in GHz after **3.5 mm** calibration

The displayed results were obtained via verification measurement with the 3.5 mm 50 Ω precision airline standard (length = 75 mm) between both measurement PORTs. The effects of the finite directivity have been removed by a time gate (gate center = 460 ps, gate span = 500 ps). Measurement results above 26.5 GHz are shown for information only.

The displayed measurement results are partly affected by the finite matching of the airline.
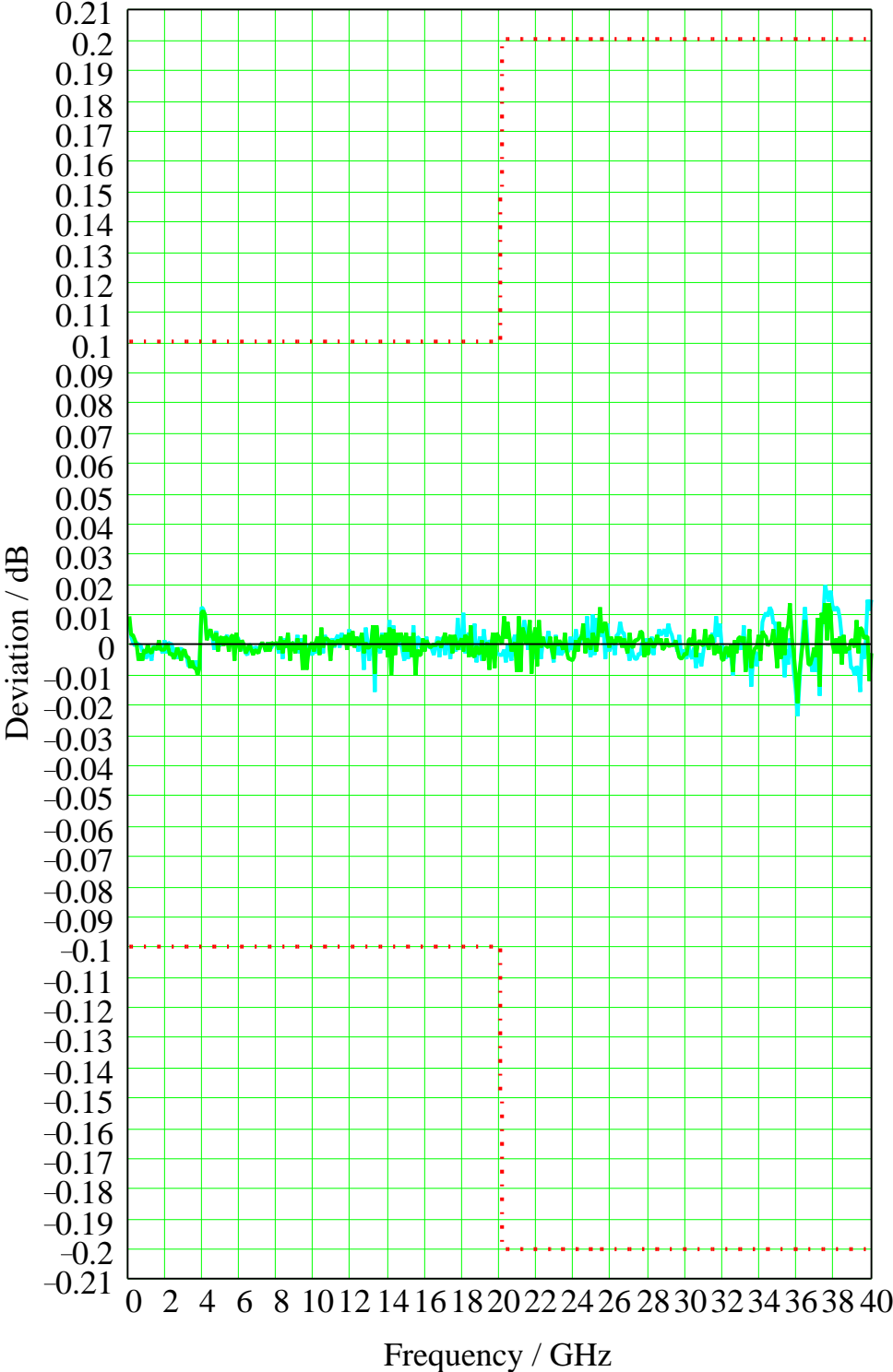
Fig. 6-18   Residual **transmission tracking** in dB vs. frequency in GHz after 2.92 mm calibration

Fig. 6-19   Residual **transmission tracking** in dB vs. frequency in GHz after 3.5 mm calibration

As pointed out earlier in this paper, the maximum useful frequency for 3.5 mm connectors is 26.5 GHz. For that reason, measurement results for frequencies greater than 26.5 GHz are presented for information only.

6 Conclusion

Accuracy is a key requirement for microwave measurements. Although the demands will differ between practical applications depending upon the specific measurement task, a high measurement accuracy is always welcome.

As has been demonstrated, the ZVK is able to perform measurements with high accuracy and stability. Systematic measurement errors can dramatically increase due to the used test setup; cables, adapters, or other components. Indeed, the measurement uncertainties can become significantly high. By using an appropriate system error calibration technique, such as the TOM-method, the systematic measurement errors are evaluated during calibration measurements. Several calibration standards are connected to the reference planes of the test setup. After finishing the calibration, the measurement accuracy can be enhanced again via numerical calculations of the system error correction technique. The calculations are performed in real-time for modern network analyzers such as the ZVK. The correction techniques enhance the effective measurement accuracy of the network analysis system to a degree, which is mainly dependent upon the quality and accuracy of the calibration standards.

7 Further Application Notes

[1] O. Ostwald: 3-Port Measurements with Vector Network Analyzer ZVR, Appl. Note 1EZ26_1E, 26 July 1996.

[2] H.-G. Krekels: Automatic Calibration of Vector Network Analyzer ZVR, Appl. Note 1EZ30_2E, 30 August 1996.

[3] O. Ostwald: 4-Port Measurements with Vector Network Analyzer ZVR, Appl. Note 1EZ25_1E, 10 October 1996.

[4] T. Bednorz: Measurement Uncertainties for Vector Network Analysis, Appl. Note 1EZ29_1E, 21 October 1996.

[5] P. Kraus: Measurements on Frequency-Converting DUTs using Vector Network Analyzer ZVR, Appl. Note 1EZ31_1E, 5 November 1996.

[6] J. Ganzert: File Transfer between Analyzers FSE or ZVR and PC using MS-DOS Interlink, Appl. Note 1EZ34_1E, 25 April 1997.

[7] J. Ganzert: Accessing Measurement Data and Controlling the Vector Network Analyzer via DDE, Appl. Note 1EZ33_1E, 28 April 1997.

[8] O. Ostwald: Group and Phase Delay Measurements with Vector Network Analyzer ZVR, Appl. Note 1EZ35_1E, 10 July 1997.

[9] O. Ostwald: Multiport Measurements using Vector Network Analyzer, Appl. Note 1EZ37_2E, 10 October 1997.

[10] O. Ostwald: Frequently Asked Questions about Vector Network Analyzer ZVR, Appl. Note 1EZ38_3E, 19 January 1998.

[11] A. Gleißner: Internal Data Transfer between Windows 3.1 / Excel and Vector Network Analyzer ZVR, Appl. Note 1EZ39_1E, 22 January 1998.

[12] A. Gleißner: Power Calibration of Vector Network Analyzer ZVR, Appl. Note 1EZ41_2E, 10 March 1998.

[13] O. Ostwald: Pulsed Measurements on GSM Amplifier SMD ICs with Vector Network Analyzer ZVR, Appl. Note 1EZ42_1E, 19 May 1998.

[14] O. Ostwald: Time Domain Measurements using Vector Network Analyzer ZVR, Appl. Note 1EZ44_0E, 19 May 1998.

[15] O. Ostwald: T-Check Accuracy Test for Vector Network Analyzers utilizing a Tee-junction, Appl. Note 1EZ43_0E, 3 June 1998.

[16] J. Simon: Virtual Embedding Networks for Vector Network Analyzer ZVR, Appl. Note 1EZ45_0E, 23 September 1998.

[17] J. Ganzert: Controlling External Generators and Power Meters with Network Analyzer ZVR, Appl. Note 1EZ46_0E, October 1998.

[18] A. Gleißner: Using the Frequency Conversion Mode of Vector Network Analyzer ZVR, Appl. Note 1EZ47_0E, 18 January 1999.

8 Ordering information

Vector Network Analyzer		
ZVK	10 MHz…40 GHz	1127.8651.60
Option Time Domain		
ZVR-B2		1044.1009.02
Test Cables		
ZV-Z15	0…40 GHz	1134.4193.02
Calibration Kit		
ZV-Z35	0…40 GHz	1128.3547.02

ROHDE & SCHWARZ